https://doi.org/10.1016/j.ijpe.2019.107570

Coordinating quality, time, and carbon emissions in perishable food production: A new technology integrating GERT and the Bayesian approach

Haiyan Wang

School of Management and E-Business, Zhejiang Gongshang University, Hangzhou 310018, China

Email: nje2010@163.com

Sha-lei Zhan*

School of Management and E-Business, Zhejiang Gongshang University, Hangzhou 310018, China

Email: zhanshalei@zjgsu.edu.cn

Tel.: +86-571-86908755

**Corresponding author.*

Chi To Ng

Logistics Research Centre, Department of Logistics and Maritime Studies, The Hong Kong Polytechnic University, Hung Hom, Kowloon, Hong Kong

Email: daniel.ng@polyu.edu.hk

T. C. E. Cheng

Logistics Research Centre, Department of Logistics and Maritime Studies, The Hong Kong Polytechnic University, Hung Hom, Kowloon, Hong Kong

Email: edwin.cheng@polyu.edu.hk

Coordinating quality, time, and carbon emissions in perishable food production: A new technology integrating GERT and the Bayesian approach

Abstract: This study concerns improving the performance of perishable food production from the joint perspective of management and technology. We consider a new idea about sustainable quality management for perishable food, which has aroused growing concern recently. Quality improvement activities (QIAs) should be carried out within the framework of the sustainable development. This motivates us to explore the tradeoffs among three sustainable metrics which involve quality, time and carbon emissions in perishable food production when optimizing QIA decision making. Our main contribution is proposing a new technology integrating Graphic Evaluation and Review Technique (GERT) and Bayesian approach, in which GERT can present the uncertainty of the three metrics and forecast their expected trends, and Bayesian approach can evaluate the probabilistic changes of the three metrics resulting from QIA decision making. To the best of our knowledge, this study is the first to use the above decision-making technology in food quality management. Furthermore, a multi-objective optimization model is built and a customized multi-objective particle swarm optimization is employed to generate the three-dimensional Pareto front to aid the decision making. We take bottled milk production as an example and present a case study on a famous Chinese dairy manufacturing firm. Numerical results and managerial insights show the advantages of our technology which include: (1) we can mitigate uncertainty, but does not change the random nature of food production; (2) we can reinforce the stability of the probabilistic change of the three metrics by increasing of the QIA-trial size; (3) we can visualize the optimal tradeoffs among the three metrics from different angles of view; and (4) we can figure out

individualized sustainable quality management plans which are node-oriented and objective-oriented. In conclusion, we hope this study can be a beneficial supplement to the quality management field of perishable food with respect to technology innovation.

Keywords: sustainability; food quality; Graphic Evaluation and Review Technique; Bayesian approach; multi-objective optimization

1. Introduction

"Perishable food" refers to food to which spoilage will quickly occur without being kept refrigerated or frozen, such as meat, dairy, seafood, and so on (Buisman et al., 2019; Chernonog and Avinadav, 2019). Perishable food supply chain (PFSC) is defined as a supply chain that concerns the processes from farm to fork with respect to perishable food (Behzadi et al., 2018; Chen et al., 2018; Utomo et al., 2018). Due to the perishable characteristics, decisions on energy-sensitive technologies and mechanical use need to be made during the supply chain activities, which entails the correlation between quality and sustainability (Stefansdottir et al., 2018). The term "sustainability", defined as the harmony among ecological, economic and social aspects, also emphasizes the waste management and resource conservation in the perishable food sector (Sgarbossa and Russo, 2017; Mangla et al., 2018). As a matter of fact, high quality can reduce perishable food loss, and further meet the social demand (Govindan, 2018; Irani et al., 2018). That is, it not only has a negative impact on the environmental issues, but also benefits the social issues (Willersinn et al., 2015; Rohmer et al., 2019). Therefore, perishable food quality, in a general sense, belongs to the broad category of sustainability (Baldwin, 2009; Akkerman et al., 2010). All these contribute to the increasing research interest in food quality management in the context of sustainability.

This study proposes a new idea about sustainable quality management in perishable food production (SQMPFP) which is a process by which the decision maker (DM) reviews the quality of all factors involved in perishable food production from the perspectives of sustainable metrics. Previous studies usually passively preserve food quality by binding quality concern with logistics and supply chain optimization problems (Zhang et al., 2003; Rong et al., 2011; Soysal et al., 2014; Sel et al., 2015; Li et al., 2016; Banasik et al., 2017; Hsiao et al., 2017; Musavi and Bozorgi-Amiri., 2017; He et al.,2018; Shankar et al.,2018; Tabrizi et al., 2018; Tsang et al., 2018). The neglect of sustainability concern also causes imperfect quality management plans. Unlike these studies, the SQMPFP, in a more active way, immediately optimizes food quality from the perspective of technical means. In fact, quality development relies on the technical means employed in the production steps rather than supply chain entities (Stefansdottir et al., 2018). Thus, there is an urgent demand to reexamine the characteristics of perishable food quality development triggered by technical means and driven by sustainable considerations.

The SQMPFP exhibits the following three characteristics. First, the quality development is shown as the generation, transfer, and integration of perishable food quality during production from the perspective of technical means, which is decided by personnel, equipment-related, raw-material, technological, and environmental factors. In terms of these factors, the decisions on quality improvement activities (QIAs) selection can be made to affect the quality of food being produced (Besik and Nagurney, 2017). For example, when cows produce raw milk, the QIA candidates include forage detecting, feeder training, antibiotics testing, as well as the combination of these single QIAs. Second, not only the production steps, but also the QIAs carried out in the production steps, demand time and energy which will result in time consumption and carbon emissions (de

Jong, 2013). However, the available time is restricted by short shelf life of perishable food (Ala-Harja and Helo, 2014; Teng et al., 2016; Feng et al., 2017; Li et al., 2017; Tiwari et al., 2018). Energy consumption is strictly limited to the low-carbon emissions (Allaoui et al., 2018; Huang et al., 2018). Therefore, there may exist possible tradeoffs among the three sustainable metrics including quality, time and carbon emissions from the perspective of the whole production process. Third, the three sustainable metrics are all under uncertainties (Rong et al., 2011; Ting et al., 2014). In respect of a production step, uncertainties emerge due to temperature- and time-sensitive nature of perishable food (Aung and Chang, 2014a; He et al., 2018). The perishability of food leads to vague resource inputs (e.g., time and energy) and quality output (Gillibert et al., 2018; Tabrizi et al., 2018). In respect of a QIA, uncertainties result from the reasonability of mechanized use and employed technologies in it (Yaseen et al., 2017). Different QIA decision making at a production step leads to different effects on quality, time and carbon emissions of the production step.

Two difficulties then arise when optimizing QIA decision making. One is the accuracy of forecasts of quality, time, and carbon emissions with stochastic nature both of production steps and QIAs. The other is the link between a production step and its possible QIA, which can figure out the probabilistic differences between pre-QIA-decision-making and post-QIA-decision-making sustainable metrics of a production step. This study proposes a novel decision-making technology which integrates Graphic Evaluation and Review Technique (GERT) and Bayesian approach, where GERT can be used to generate measures of presenting the uncertainty of the three sustainable metrics during perishable food production and forecast their expected trends, and Bayesian approach can evaluate the dynamic changes of sustainable metrics of all production steps resulting from QIA decision making. To the best of our knowledge, this study is the first to use the above

decision-making technology in food quality management. Furthermore, this study builds a multi-objective optimization model to search for the best tradeoffs among the three sustainable metrics.

The rest of the paper is organized as follows. Section 2 reviews the literature. Section 3 presents the Bayesian-updated GERT. Section 4 proposes a multi-objective model and its solution approach. Section 5 shows the computational results and insights. Section 6 states the conclusions.

2. Literature Review

2.1. Perishable food quality

Works related to perishable food quality have been conducted on different levels. From the perspective of the whole PFSC, researches by Aung and Chang (2014b) and Shankar et al. (2018) both develop a traceability system, whereas the study by Dania et al. (2018) highlights the supply chain collaboration. Aiming at some segments of PFSC or the sub-problems of PFSC optimization, studies preserve perishable food quality in location-allocation problems (Zhang et al., 2003; Musavi and Bozorgi-Amiri, 2017; Jonkman et al., 2019), routing-allocation problems (Soysal et al., 2014; Tsang et al., 2018), production-distribution problems (Rong et al., 2011; Sel et al., 2015; Li et al., 2016; Banasik et al., 2017), pricing-inventory problems (Teng et al., 2016; Feng et al., 2017; Li et al., 2017; Tabrizi et al., 2018; Tiwari et al., 2018), and customer behavior problems (Aschemann-Witzel et al., 2018; He et al.,2018; Singh et al.,2018; Yoo and Cheong, 2018). In addition, micro-level studies are also recommended by designing the multi-temperature storing space for transport vehicles (Hsiao et al., 2017), determining an optimum target temperature range for refrigerated storage (Aung and Chang, 2014a; de Frias et al., 2018; Ndraha et al., 2018), and adopting edible coating or packaging to protect the perishable foods (Arnon-Rips and Poverenov,

2018; Bortolini et al., 2018). However, several limitations exist in the above studies:

- Perishable food quality management is treated as a passive concept.
- Perishable food quality is addressed without sustainable consideration.
- The positive effect of perishable food quality on sustainability is ignored.
- Quality management is addressed more from the management than from the technology perspective.

2.2. Quality uncertainty and dynamics

Being aware of that the quality degradation of perishable food depends on time and temperature, researches address dynamics of food quality by using quality degradation equations (Zhang et al., 2003), proposing a minimum residual shelf life and quality control time (Sel et al., 2015), defining a quality level index to trace the quality decrease (Li et al., 2016; Jonkman et al., 2019), and characterizing quality level by a stepped decrease function with time (Musavi and Bozorgi-Amiri, 2017; Hsiao et al., 2017). The first commonality among the above studies lies in that the dynamics of food quality addressed are only driven by the self-nature of perishable food, few studies have paid attention to dynamics triggered by external factors, such as QIA decision making. Second is that most studies formulate the dynamics of food quality without considering uncertainty. Although Rong et al. (2011) consider that the expected quality at given time periods and temperatures can demonstrate the trend of quality degradation, the quality uncertainty has not yet been really targeted. A few researches try to use sampling tests to distinguish whether the food conforms to the quality specification (Chen et al., 2014; Sader et al., 2018) or whether the food is contaminated (Chebolu-Subramanian and Gaukler, 2015), but the uncertainty in these articles has not involved the quality dynamics. Therefore, the combined consideration of quality uncertainty and

dynamics of perishable food is rare.

2.3. Multi-objective optimization

When developing objectives for optimization models, cost or profit is a common metric due to the commercial nature of perishable food (Zhang et al., 2003; Rong et al., 2011; Sel et al., 2015; Li et al., 2016; Hsiao et al., 2017; Jonkman et al., 2017; Albornoz and Urrutia–Gutiérrez, 2018; Aras and Bilge, 2018; Mogale et al., 2018b). According to Table 1, numerous studies put forward other metrics, such as temporal, social, and environmental impacts. To coordinate these conflicting metrics, multi-objective modelling is employed by Govindan et al. (2014), Soysal et al. (2014), Banasik et al. (2017), Miranda-Ackerman et al. (2017), Musavi and Bozorgi-Amiri (2017), Allaoui et al. (2018), Bortolini et al. (2018), Jonkman et al. (2019), Mogale et al. (2018a), Tsang et al. (2018), Jonkman et al. (2019), and Rohmer et al. (2019). The common limitations of them are:

- Perishable food quality maximization has not yet been pursued as an independent goal.
- Little research considers perishable food quality as a sustainable metric.
- The relationships between the quality and other sustainable metrics have not yet been explored.

In addition, the Pareto front is necessary in multi-objective problems (Ehrgott, 2005). This study respects the existing approaches, such as ε-constraint method (Soysal et al., 2014; Banasik et al., 2017; Allaoui et al., 2018; Rohmer et al., 2019), normalized normal constraint method (Bortolini et al., 2018), genetic algorithm (Miranda-Ackerman et al., 2017; Musavi and Bozorgi-Amiri, 2017; Kowalski et al., 2018; Tsang et al., 2018), and particle swarm optimization (Govindan et al., 2014; Tabrizi et al., 2018), but we employ a customized particle swarm optimization algorithm to fit our model.

Table 1 A summary of relevant works

Paper	*Topic*	*Sustainability*	*Quality control*	*Uncertainty of quality*	*Dynamics of quality*	*Multiple objectives*	*Objectives details*	*Solution method*
Zhang et al. (2003)	Location-allocation for cold chain		√		√		Cost	Meta-heuristic
Rong et al. (2011)	Production and distribution for food supply chain		√	√	√		Cost	Exact approach
Govindan et al. (2014)	Location–routing for perishable food supply chain network	√				√	Cost, environmental impact	Meta-heuristic
Soysal et al. (2014)	Vehicle routing, resource allocation for beef transportation	√	√			√	Cost, carbon emission	Exact approach
Sel et al. (2015)	Production and distribution for dairy supply chain		√		√		Cost	Meta-heuristic
Li et al. (2016)	Production and distribution for perishable food		√		√		profit	Exact approach
Banasik et al. (2017)	Production and distribution in food supply chain	√	√			√	Cost, environmental impact	Exact approach
Hsiao et al. (2017)	Resource allocation for cold chain		√		√		Cost	Meta-heuristic
Jonkman et al. (2017)	Location-allocation for food process design						Profit	Exact approach
Miranda-Ackerman et al. (2017)	Agro-food supply chain network design	√				√	Cost, environmental impact	Meta-heuristic
Musavi and Bozorgi-Amiri (2017)	Facility location, vehicle routing for food supply chain	√	√		√	√	Cost, quality, carbon emission	Meta-heuristic
Allaoui et al. (2018)	Agro-food supply chain network design	√				√	Cost, environmental and social goal, efficiency	Exact approach
Albornoz and Urrutia–Gutiérrez (2018)	Crop resource allocation						Profit	Exact approach
Aras and Bilge (2018)	Location-allocation for food supply chain network						Cost	Exact approach
Bortolini et al. (2018)	Location-allocation for closed loop food distribution network	√				√	Cost, environmental impact	Exact approach
Mogale et al. (2018a)	Location-allocation for food grain supply chain					√	Cost, lead time	Meta-heuristic
Mogale et al. (2018b)	Food transportation and storage for food grain supply chain						Cost	Meta-heuristic
Tabrizi et al. (2018)	Food supply and inventory policy	√	√		√	√	Total profit of leader, total profit of follower	Meta-heuristic
Tsang et al. (2018)	Vehicle routing and resource allocation for food distribution		√			√	Cost, time	Meta-heuristic
Jonkman et al. (2019)	Location-allocation for crop production and harvest	√	√		√	√	Profit, environmental impact	Exact approach
Rohmer et al. (2019)	Production and distribution for food network design	√				√	Cost, environmental impact	Exact approach

2.4. Research gaps

In summary, this study aims at filling the gaps in the existing literatures.

First, this study is the first attempt to immediately optimize perishable food quality from the joint perspective of management and technology, and under sustainable consideration.

Second, we pay attention to the neglect of combined consideration of dynamics and uncertainty in perishable food production. We are the first attempt to propose a novel technology by integrating GERT and Bayesian approach to show the joint dynamic uncertainty.

Third, we develop a multi-objective model to pursue quality together with the other two sustainable metrics. To the best of our knowledge, balancing the triple objectives simultaneously is also rare among the existing relevant works.

3. Technology of Bayesian-updated GERT for SQMPFP

3.1. Networks of perishable food production: A bottled milk case

Dairy product is a typical product within the category of perishable food (Sel et al., 2015). It is heated and cooled many times to maintain its quality during its production, which requires various combinations of time- and energy-sensitive technologies to show quality in different sustainable metrics (de Jong, 2013; Stefansdottir et al., 2018). This motivates us to focus on production technology optimization of this product type. We address an SQMPFP problem on dairy product production based on a centralized chain structure. Centralization refers to the situation where decisions in a production chain are made by a single DM who has all information at hand (Chen et al., 2014). We have identified that in eastern China, there are several famous dairy manufacturing firms with centralized chain structures, such as Beingmate, Bright Dairy, and New Hope. They manage their own farms and complete production lines, and adopt vertical strategies with quality

control. In this study, we concentrate on the production steps of a typical dairy product, namely bottled milk (see Fig. 1), based on our survey of these companies. The production process before the filled milk consists of three sub-steps: sterilized milk processing, auxiliary materials concocting and bottles preparation. Reprocessing is only allowed in the latter two sub-steps, because the unqualified milk must be abandoned absolutely to comply with the national food safety standard. Both auxiliary materials recycling and bottles recycling are recommended so that the whole production process forms a sustainable network structure.

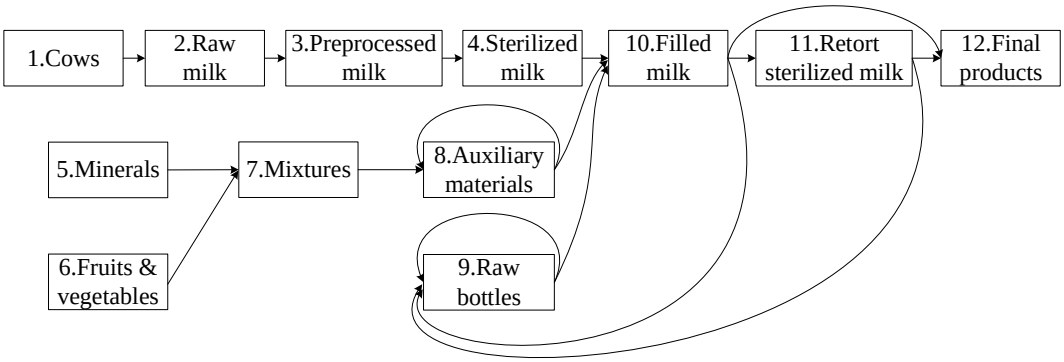

Fig. 1 The sequence of production steps of bottled milk

During the production of bottled milk, the resource input and quality output cannot be deterministically determined as they are uncertain quantities (Gillibert et al., 2018; Stefansdottir et al., 2018; Tabrizi et al., 2018). Based on sequential production steps, a stochastic network is drawn to show the randomness and dynamics during the product form transitions (see Fig. 2a). A node represents a product form. Twelve product forms are respectively designated with nodes numbered Nodes 1 to 12. The disposal node exists in reality but is omitted here due to the space of figure. An arc represents a possible product form transition. Define that i is an arbitrary node in the network, $i = 1, 2, \cdots, I$, where I is the number of nodes in the network; (i, j) is an arc emitted from node i, and j is a node next to node i, $j \in A_i$, where A_i is the set of all successor nodes of node i and $J_i = |A_i|$. The quality outputted by node i is represented by $\boldsymbol{p_i} = (p_{i1}, p_{i2}, \cdots, p_{iJ_i})^T$ which

follows a Dirichlet distribution, i.e., $\boldsymbol{p_i}\sim Dir(\boldsymbol{\alpha_i})$, where p_{ij} is the quality outputted from node i to its j th successor node (arranged in ascending order of node numbers), and $\boldsymbol{\alpha_i} = (\alpha_{i1}, \alpha_{i2}, \cdots, \alpha_{iJ_i})^T$ can be estimated by historical quality data. Furthermore, producing quality products needs time and carbon emissions. It seems not difficult to time each production step and estimate the corresponding carbon emissions. Nowadays, the traceability system has been developed to time and visualize food producing in many Chinese companies (Wang and Yue, 2017; Wang et al., 2017; Shen et al., 2018). The carbon emissions can also be estimated by electricity and fuel consumption (de Jong, 2013; Soysal et al., 2014). But they are still under uncertainty and correlated with each other. Therefore, we define that time q_{ij} and carbon emissions r_{ij} on each arc respectively follow normal distributions, i.e., $q_{ij}\sim N(\mu_{ij1}, \sigma_{ij1}^2)$, $r_{ij}\sim N(\mu_{ij2}, \sigma_{ij2}^2)$. The combination of them follows a bivariate normal distribution, denoted as $\mathbf{K_{ij}}\sim N(\boldsymbol{\mu_{ij}}, \boldsymbol{\Sigma_{ij}})$, where $\mathbf{K_{ij}} = \begin{pmatrix} q_{ij} \\ r_{ij} \end{pmatrix}$, $\boldsymbol{\mu_{ij}} = \begin{pmatrix} \mu_{ij1} \\ \mu_{ij2} \end{pmatrix}$, $\boldsymbol{\Sigma_{ij}} = \begin{pmatrix} \sigma_{ij1}^2 & \rho_{ij}\sigma_{ij1}\sigma_{ij2} \\ \rho_{ij}\sigma_{ij1}\sigma_{ij2} & \sigma_{ij2}^2 \end{pmatrix}$, and ρ_{ij} is the correlation between q_{ij} and r_{ij}. Therefore, the uncertainties of a stochastic network have been quantified by arc parameters $(p_{ij}, \mathbf{K_{ij}^T})$.

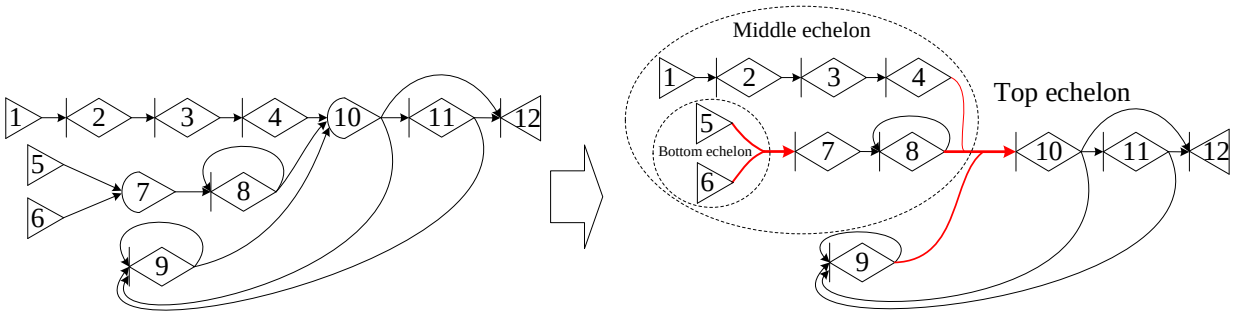

(a) A stochastic network for bottled milk production

(b) Equivalent three-echelon GERT networks for bottled milk production

Fig. 2 Transformation from stochastic network to GERT networks

In a general stochastic network, there are three types of input (i.e., XOR, OR and AND) and two types of output (i.e., Deterministic and Non-deterministic), resulting in six types of node logic,

denoted as ⋈ (XOR & Deterministic), ⋈ (XOR & Non-deterministic), ◇ (OR & Deterministic), ◇ (OR & Non-deterministic), ○ (AND & Deterministic), and ○ (AND & Non-deterministic) (Zhou et al., 2016; Nelson et al., 2016). However, a GERT network only considers one input node logic, i.e., XOR (Pritsker, 1966). Therefore, we follow an equivalent transformation criterion to draw equivalent three-echelon GERT networks for Fig. 2a which results in Fig. 2b. Both in bottom- and middle-echelon networks, the AND types are replaced by XOR types, on the premise of regarding the network in an echelon as a whole, and outputting an equivalent integrated arc. The details will be shown in Section 4.1.

Not only the uncertainty, but also the dynamics are taken into consideration when analyzing the effects on GERT networks by QIA decision making. Define that ω_{im} represents the mth QIA in node i, $m = 1, 2, \cdots, \Omega_i$, where Ω_i is the number of QIAs in node i. Whether a QIA is carried out or not in a node will immediately affect the quality, time and carbon emissions of the arcs outputted by this node (Note that here we only consider the carbon emissions associated with electricity and fuel consumption, because the carbon footprint of a QIA mainly results from electricity and fuel use). For example, when cows produce raw milk, a QIA named "milking by machines" is carried out. Then it improves the milk quality, saves the milking time, and certainly increases carbon emissions. However, the effect caused by QIA decision making is probabilistic, and it will not change the random nature of GERT networks. Bayesian approach, as a popular tool in Statistics, is used to update the probability of an event when more information becomes available (Zhan et al., 2014; Zhan and Liu, 2016). In this study, we regard carrying out a QIA as providing the arc parameters with "more information". Therefore, the GERT networks updated by QIA decision making are obviously more complicated than the ones without update.

3.2. Bayesian updates of arc parameters

The DM needs to decide whether or not to locate a node to carry out a QIA, as well as whether or not to allocate a QIA to it. We define two types of decision variables: one is location variable z_i, which is equal to 1 if node i is located, and 0, otherwise; the other is allocation variable x_{im}, which is equal to 1 if QIA ω_{im} is carried out in node i, and 0, otherwise. Then the relationship between the two types of decision variables is formulated as

$$\sum_m x_{im} = z_i. \tag{1}$$

Different QIA strategies lead to different updates of arc parameters. We call the arc parameters $(p_{ij}, \mathbf{K_{ij}^T})$ original parameters. Differently, we call the arc parameters affected by QIA decision making as updated parameters, and denote them as $(\pi_{ij}, \mathbf{H_{ij}^T})$ where $\mathbf{H_{ij}} = \begin{pmatrix} t_{ij} \\ c_{ij} \end{pmatrix}$.

When a QIA is carried out in a node, QIA characteristics including effectiveness, time and carbon emissions are under uncertainty. Therefore, numerous QIA trials are needed to simulate these uncertain characteristics. Then, the Bayesian approach is employed to update the arc parameters in the GERT networks based on the observations of the QIA trials.

3.2.1. Bayesian update of arc probability

As aforementioned, the original arc probability means the original quality outputted by node i. It follows a Dirichlet distribution $\boldsymbol{p_i} \sim Dir(\boldsymbol{\alpha_i})$. Suppose that from the long-term perspective, the arc probability affected by an effective QIA also follows a Dirichlet distribution, and is denoted as $\boldsymbol{s_{im}} \sim Dir(\boldsymbol{\lambda_{im}\alpha_i})$, where $\boldsymbol{s_{im}} = \left(s_{im1}, s_{im2}, \cdots, s_{imJ_i}\right)^T$, $\boldsymbol{\lambda_{im}} = \begin{pmatrix} \lambda_{im1} & 0 & 0 \\ 0 & \ddots & 0 \\ 0 & 0 & \lambda_{imJ_i} \end{pmatrix}$. $\boldsymbol{\lambda_{im}}$ is a coefficient representing the promoting degree of the original arc probability. To our knowledge, a QIA is not always effective and sometimes may lose its effectiveness, which indicates that the effectiveness of a QIA is also under uncertainty. In terms of a single QIA trial, whether or not a QIA

can successfully change the arc probability seems like a categorical trial. Suppose that there are N_{im} trials of QIA ω_{im}. Therefore, the effectiveness of QIA ω_{im} in all N_{im} QIA trials follows a multinomial distribution denoted as $\boldsymbol{e_{im}}|\boldsymbol{s_{im}} \sim MN(N_{im}, \boldsymbol{s_{im}})$. $\boldsymbol{e_{im}}$ can be rewritten as $\boldsymbol{e_{im}} = (\boldsymbol{e_{im1}}, \boldsymbol{e_{im2}}, \cdots, \boldsymbol{e_{imN_{im}}}) = \begin{pmatrix} e_{im11} & \cdots & e_{im1N_{im}} \\ \vdots & \ddots & \vdots \\ e_{imJ_i1} & \cdots & e_{imJ_iN_{im}} \end{pmatrix}$. All the sub-vectors of $\boldsymbol{e_{im}}$ are $J_i \times 1$ vectors filled with 0-1 numbers. For example, $\boldsymbol{e_{im2}} = \begin{pmatrix} e_{im12} \\ \vdots \\ e_{imJ_i2} \end{pmatrix} = \begin{pmatrix} 1 \\ 0 \\ \vdots \end{pmatrix}$ means that the quality outputted by node i goes to the first subsequent node in the second trial of QIA ω_{im}.

By borrowing the property of conjugate family (Berger, 1985), we can infer that the Dirichlet distribution is conjugate to itself with respect to a multinomial likelihood function. Then, by using the Bayes' theorem, the posterior arc probability outputted by node i is

$$\boldsymbol{s_{im}}|\boldsymbol{e_{im}} \sim Dir\left(\lambda_{im1}\alpha_{i1} + \sum_n e_{im1n}, \cdots, \lambda_{imJ_i}\alpha_{iJ_i} + \sum_n e_{imJ_in}\right). \quad (2)$$

Then, the updated arc probability outputted by node i affected by QIA decision making is

$$\pi_{ij} = \begin{cases} \sum_m \left(x_{im} E\left(s_{imj}|\boldsymbol{e_{im}}\right)\right), if\ z_i = 1, \\ E\left(p_{ij}\right), if\ z_i = 0. \end{cases} \quad (3)$$

$E\left(s_{imj}|\boldsymbol{e_{im}}\right)$ can be calculated by an important property of Dirichlet distribution which results in $E\left(s_{imj}|\boldsymbol{e_{im}}\right) = \frac{\lambda_{imj}\alpha_{ij} + \sum_n e_{imjn}}{\sum_j (\lambda_{imj}\alpha_{ij} + \sum_n e_{imjn})}$. Eq. (3) integrates QIA decision making and Bayesian updates. If carrying out a QIA (i.e., $z_i = 1$ and a certain $x_{im} = 1$), the righthand side of Eq. (3) is equal to the expected value of posterior arc probability. If no QIA is carried out (i.e., $z_i = 0$ and each $x_{im} = 0$), the righthand side of Eq. (3) is equal to the expected value of the original arc probability.

3.2.2. Bayesian updates of both arc time and arc carbon emissions

The updates of the arc time and arc carbon emissions obviously differ from the arc probability.

Time and carbon emissions are always consumed in spite of the uncertainty of QIA effectiveness. As aforementioned, time q_{ij} and carbon emissions r_{ij} follow normal distributions, i.e., $q_{ij}\sim N(\mu_{ij1},\sigma_{ij1}^2)$, $r_{ij}\sim N(\mu_{ij2},\sigma_{ij2}^2)$, and $\mathbf{K_{ij}}\sim N(\boldsymbol{\mu_{ij}},\boldsymbol{\Sigma_{ij}})$. Based on the common assumptions in the real-world practice, a QIA's time t'_{im} and carbon emissions c'_{im} also follow similar distributions, i.e., $\boldsymbol{\kappa_{im}}\sim N(\boldsymbol{\Theta_{im}},\mathbf{T_{im}})$, where $\boldsymbol{\kappa_{im}}=\begin{pmatrix}t'_{im}\\c'_{im}\end{pmatrix}$, $\boldsymbol{\Theta_{im}}=\begin{pmatrix}\theta_{im1}&0\\0&\theta_{im2}\end{pmatrix}$, $\mathbf{T_{im}}=\begin{pmatrix}\tau_{im1}^2&\nu_{im}\tau_{im1}\tau_{im2}\\\nu_{im}\tau_{im1}\tau_{im2}&\tau_{im2}^2\end{pmatrix}$, and ν_{im} is the correlation between t'_{im} and c'_{im}. It is very important to note that t'_{im} is related to q_{ij}, and c'_{im} is related to r_{ij}. Generally, t'_{im} accounts for a proportion of q_{ij}, c'_{im} accounts for a proportion of r_{ij}. Then, the relationship is formulated as a likelihood function, i.e.,

$$\boldsymbol{\kappa_{im}}|\mathbf{K_{ij}}\sim N(\boldsymbol{\Theta_{im|ij}}\mathbf{K_{ij}},\mathbf{T_{im|ij}}), \tag{4}$$

where $\boldsymbol{\kappa_{im}}|\mathbf{K_{ij}}=\begin{pmatrix}t'_{im}|\mathbf{K_{ij}}\\c'_{im}|\mathbf{K_{ij}}\end{pmatrix}$, $\boldsymbol{\Theta_{im|ij}}=\begin{pmatrix}\theta_{im1|ij}&0\\0&\theta_{im2|ij}\end{pmatrix}$, $\mathbf{T_{im|ij}}=\begin{pmatrix}\tau_{im1|ij}^2&\nu_{im|ij}\tau_{im1|ij}\tau_{im2|ij}\\\nu_{im|ij}\tau_{im1|ij}\tau_{im2|ij}&\tau_{im2|ij}^2\end{pmatrix}$, and $\nu_{im|ij}$ is the correlation between t'_{im} and c'_{im} given $\mathbf{K_{ij}}$.

Then, by borrowing again the property of conjugate family (Berger, 1985), we can infer that the Gaussian family is conjugate to itself with respect to a Gaussian likelihood function. Therefore, by using the Bayes' theorem, we can obtain

$$\mathbf{K_{ij}}|\bar{\boldsymbol{\kappa}}_{\boldsymbol{im}}\sim N\left(\boldsymbol{\Theta}_{\boldsymbol{im|ij}}^{-\mathbf{1}}\boldsymbol{\Phi_{ij|im}},\boldsymbol{\Theta}_{\boldsymbol{im|ij}}^{-\mathbf{1}}\boldsymbol{\Psi_{ij|im}}\left(\boldsymbol{\Theta}_{\boldsymbol{im|ij}}^{-\mathbf{1}}\right)^{\mathbf{T}}\right), \tag{5}$$

where $\bar{\boldsymbol{\kappa}}_{\boldsymbol{im}}=\begin{pmatrix}\frac{\sum_n \hat{t}'_{imn}}{N_{im}}\\\frac{\sum_n \hat{c}'_{imn}}{N_{im}}\end{pmatrix}$ is the sample mean of $\boldsymbol{\kappa_{im}}$ observed in all N_{im} QIA trials, $\hat{t}'_{imn}$ and $\hat{c}'_{imn}$ respectively represent sample time and carbon emissions in the nth QIA trial, $\mathbf{K_{ij}}|\bar{\boldsymbol{\kappa}}_{\boldsymbol{im}}=\begin{pmatrix}q_{ij}|\bar{\boldsymbol{\kappa}}_{\boldsymbol{im}}\\r_{ij}|\bar{\boldsymbol{\kappa}}_{\boldsymbol{im}}\end{pmatrix}$,

$$\boldsymbol{\Phi_{ij|im}}=\boldsymbol{\Psi_{ij|im}}\left(\left(\boldsymbol{\Theta_{im|ij}}\boldsymbol{\Sigma_{ij}}\boldsymbol{\Theta}_{\boldsymbol{im|ij}}^{\mathbf{T}}\right)^{-\mathbf{1}}\boldsymbol{\Theta_{im|ij}}\boldsymbol{\mu_{ij}}+N_{im}\mathbf{T}_{\boldsymbol{im|ij}}^{-\mathbf{1}}\bar{\boldsymbol{\kappa}}_{\boldsymbol{im}}\right), \tag{6}$$

and

$$\boldsymbol{\Psi}_{ij|im} = \left(\left(\boldsymbol{\Theta}_{im|ij}\boldsymbol{\Sigma}_{ij}\boldsymbol{\Theta}_{im|ij}^{\mathbf{T}}\right)^{-1} + N_{im}\mathbf{T}_{im|ij}^{-1}\right)^{-1}. \quad (7)$$

Proof:

First, by borrowing Corollary B.5 of Bijma et al. (2017), we can infer

$$\boldsymbol{\Theta}_{im|ij}\mathbf{K}_{ij} \sim N\left(\boldsymbol{\Theta}_{im|ij}\boldsymbol{\mu}_{ij}, \boldsymbol{\Theta}_{im|ij}\boldsymbol{\Sigma}_{ij}\boldsymbol{\Theta}_{im|ij}^{\mathbf{T}}\right). \quad (8)$$

Second, according to Eq. (4), the likelihood function is

$$\bar{\boldsymbol{\kappa}}_{im}\left|\boldsymbol{\Theta}_{im|ij}\mathbf{K}_{ij} = \bar{\boldsymbol{\kappa}}_{im}\right|\mathbf{K}_{ij} = N\left(\boldsymbol{\Theta}_{im|ij}\mathbf{K}_{ij}, N_{im}^{-1}\mathbf{T}_{im|ij}\right). \quad (9)$$

Third, by referring to page 400 of Bolstad and Curran (2017), we can obtain

$$\boldsymbol{\Theta}_{im|ij}\mathbf{K}_{ij}|\bar{\boldsymbol{\kappa}}_{im} \sim N\left(\boldsymbol{\Phi}_{ij|im}, \boldsymbol{\Psi}_{ij|im}\right), \quad (10)$$

where $\boldsymbol{\Phi}_{ij|im}$ and $\boldsymbol{\Psi}_{ij|im}$ are respectively shown in Eqs. (6) and (7).

Therefore, Eq. (5) can be calculated by borrowing Corollary B.5 of Bijma et al. (2017) again.

□

Property 1. The posterior mean $E\left(\mathbf{K}_{ij}|\bar{\boldsymbol{\kappa}}_{im}\right)$ is the weighted sum of the prior mean $E\left(\mathbf{K}_{ij}\right)$ and the coefficient-multiplied sample mean (CMSM) $\boldsymbol{\Theta}_{im|ij}^{-1}\bar{\boldsymbol{\kappa}}_{im}$.

Proof:

First,

$$\begin{aligned}\boldsymbol{\Theta}_{im|ij}^{-1}\boldsymbol{\Psi}_{ij|im} &= \boldsymbol{\Theta}_{im|ij}^{-1}\left(\left(\boldsymbol{\Theta}_{im|ij}\boldsymbol{\Sigma}_{ij}\boldsymbol{\Theta}_{im|ij}^{\mathbf{T}}\right)^{-1} + N_{im}\mathbf{T}_{im|ij}^{-1}\right)^{-1} \\ &= \left(\left(\left(\boldsymbol{\Theta}_{im|ij}\boldsymbol{\Sigma}_{ij}\boldsymbol{\Theta}_{im|ij}^{\mathbf{T}}\right)^{-1} + N_{im}\mathbf{T}_{im|ij}^{-1}\right)\boldsymbol{\Theta}_{im|ij}\right)^{-1} \\ &= \left(\left(\boldsymbol{\Sigma}_{ij}\boldsymbol{\Theta}_{im|ij}^{\mathbf{T}}\right)^{-1} + \left(N_{im}\mathbf{T}_{im|ij}^{-1}\boldsymbol{\Theta}_{im|ij}\right)\right)^{-1}.\end{aligned}$$

Second,

$$\begin{aligned}E\left(\mathbf{K}_{ij}|\bar{\boldsymbol{\kappa}}_{im}\right) &= \boldsymbol{\Theta}_{im|ij}^{-1}\boldsymbol{\Phi}_{ij|im} \\ &= \boldsymbol{\Theta}_{im|ij}^{-1}\boldsymbol{\Psi}_{ij|im}\left(\left(\boldsymbol{\Theta}_{im|ij}\boldsymbol{\Sigma}_{ij}\boldsymbol{\Theta}_{im|ij}^{\mathbf{T}}\right)^{-1}\boldsymbol{\Theta}_{im|ij}\boldsymbol{\mu}_{ij} + N_{im}\mathbf{T}_{im|ij}^{-1}\bar{\boldsymbol{\kappa}}_{im}\right)\end{aligned}$$

$$= \left(\left(\boldsymbol{\Sigma}_{ij}\boldsymbol{\Theta}_{im|ij}^{\mathbf{T}}\right)^{-1} + \left(N_{im}\mathbf{T}_{im|ij}^{-1}\boldsymbol{\Theta}_{im|ij}\right)\right)^{-1}\left(\left(\boldsymbol{\Sigma}_{ij}\boldsymbol{\Theta}_{im|ij}^{\mathbf{T}}\right)^{-1}\boldsymbol{\mu}_{ij} + \left(N_{im}\mathbf{T}_{im|ij}^{-1}\boldsymbol{\Theta}_{im|ij}\right)\boldsymbol{\Theta}_{im|ij}^{-1}\bar{\boldsymbol{\kappa}}_{im}\right). \quad (11)$$

According to Eq. (11), Property 1 is proved. The weights are respectively $\left(\left(\boldsymbol{\Sigma}_{ij}\boldsymbol{\Theta}_{im|ij}^{\mathbf{T}}\right)^{-1} + \left(N_{im}\mathbf{T}_{im|ij}^{-1}\boldsymbol{\Theta}_{im|ij}\right)\right)^{-1}\left(\boldsymbol{\Sigma}_{ij}\boldsymbol{\Theta}_{im|ij}^{\mathbf{T}}\right)^{-1}$ and $\left(\left(\boldsymbol{\Sigma}_{ij}\boldsymbol{\Theta}_{im|ij}^{\mathbf{T}}\right)^{-1} + \left(N_{im}\mathbf{T}_{im|ij}^{-1}\boldsymbol{\Theta}_{im|ij}\right)\right)^{-1}\left(N_{im}\mathbf{T}_{im|ij}^{-1}\boldsymbol{\Theta}_{im|ij}\right)$. □

Property 2. The posterior variance $V\left(\mathbf{K}_{ij}|\bar{\boldsymbol{\kappa}}_{im}\right)$ depends on the prior variance $V\left(\mathbf{K}_{ij}\right)$ and the likelihood variance $V\left(\boldsymbol{\Theta}_{im|ij}^{-1}\bar{\boldsymbol{\kappa}}_{im}\middle|\mathbf{K}_{ij}\right)$. Precisely,

$$\left(V\left(\mathbf{K}_{ij}|\bar{\boldsymbol{\kappa}}_{im}\right)\right)^{-1} = \left(V\left(\mathbf{K}_{ij}\right)\right)^{-1} + \left(V\left(\boldsymbol{\Theta}_{im|ij}^{-1}\bar{\boldsymbol{\kappa}}_{im}\middle|\mathbf{K}_{ij}\right)\right)^{-1}. \quad (12)$$

Proof:

First, $\boldsymbol{\Theta}_{im|ij} = \boldsymbol{\Theta}_{im|ij}^{\mathbf{T}} = \begin{pmatrix}\theta_{im1|ij} & 0\\ 0 & \theta_{im2|ij}\end{pmatrix}$, $\boldsymbol{\Theta}_{im|ij}^{-1} = \left(\boldsymbol{\Theta}_{im|ij}^{-1}\right)^{T} = \begin{pmatrix}\frac{1}{\theta_{im1|ij}} & 0\\ 0 & \frac{1}{\theta_{im2|ij}}\end{pmatrix}$.

Second, $V\left(\bar{\boldsymbol{\kappa}}_{im}\middle|\mathbf{K}_{ij}\right) = N_{im}^{-1}\mathbf{T}_{im|ij}$ according to Eq. (9), then

$$V\left(\boldsymbol{\Theta}_{im|ij}^{-1}\bar{\boldsymbol{\kappa}}_{im}\middle|\mathbf{K}_{ij}\right) = N_{im}^{-1}\boldsymbol{\Theta}_{im|ij}^{-1}\mathbf{T}_{im|ij}\left(\boldsymbol{\Theta}_{im|ij}^{-1}\right)^{T}$$

$$= N_{im}^{-1}\boldsymbol{\Theta}_{im|ij}^{-1}\mathbf{T}_{im|ij}\boldsymbol{\Theta}_{im|ij}^{-1}$$

$$= \left(N_{im}\boldsymbol{\Theta}_{im|ij}\mathbf{T}_{im|ij}^{-1}\boldsymbol{\Theta}_{im|ij}\right)^{-1},$$

therefore, $\left(V\left(\boldsymbol{\Theta}_{im|ij}^{-1}\bar{\boldsymbol{\kappa}}_{im}\middle|\mathbf{K}_{ij}\right)\right)^{-1} = N_{im}\boldsymbol{\Theta}_{im|ij}\mathbf{T}_{im|ij}^{-1}\boldsymbol{\Theta}_{im|ij}$.

Third, $V\left(\mathbf{K}_{ij}|\bar{\boldsymbol{\kappa}}_{im}\right) = \boldsymbol{\Theta}_{im|ij}^{-1}\boldsymbol{\Psi}_{ij|im}\left(\boldsymbol{\Theta}_{im|ij}^{-1}\right)^{\mathbf{T}}$

$$= \left(\left(\boldsymbol{\Sigma}_{ij}\boldsymbol{\Theta}_{im|ij}^{\mathbf{T}}\right)^{-1} + \left(N_{im}\mathbf{T}_{im|ij}^{-1}\boldsymbol{\Theta}_{im|ij}\right)\right)^{-1}\boldsymbol{\Theta}_{im|ij}^{-1}$$

$$= \left(\boldsymbol{\Theta}_{im|ij}\left(\boldsymbol{\Sigma}_{ij}\boldsymbol{\Theta}_{im|ij}^{\mathbf{T}}\right)^{-1} + \left(N_{im}\boldsymbol{\Theta}_{im|ij}\mathbf{T}_{im|ij}^{-1}\boldsymbol{\Theta}_{im|ij}\right)\right)^{-1}$$

$$= \left(\boldsymbol{\Sigma}_{ij}^{-1} + \left(N_{im}\boldsymbol{\Theta}_{im|ij}\mathbf{T}_{im|ij}^{-1}\boldsymbol{\Theta}_{im|ij}\right)\right)^{-1}$$

$$= \left(\left(V\left(\mathbf{K}_{ij}\right)\right)^{-1} + \left(V\left(\boldsymbol{\Theta}_{im|ij}^{-1}\bar{\boldsymbol{\kappa}}_{im}\middle|\mathbf{K}_{ij}\right)\right)^{-1}\right)^{-1}.$$

Therefore, Eq. (12) is proved. □

Then, according to Eq. (12), we can infer $\left(V\left(\mathbf{K}_{ij}|\bar{\boldsymbol{\kappa}}_{im}\right)\right)^{-1} > \left(V\left(\mathbf{K}_{ij}\right)\right)^{-1}$. Therefore,

$$V\left(\mathbf{K}_{ij}|\bar{\boldsymbol{\kappa}}_{im}\right) < V\left(\mathbf{K}_{ij}\right). \quad (13)$$

Furthermore, we can infer that the smaller the likelihood variance is, the greater the gap between the prior variance and the posterior variance will be. Because the likelihood variance is inversely proportional to the QIA-trial size, the increase of QIA-trial size will broaden the gap between the prior variance and the posterior variance.

Then the updated time and carbon emissions of an arc affected by QIA decision making are integrated into

$$\mathbf{H}_{ij} = \begin{cases} \sum_m \left(x_{im} \mathbf{K}_{ij} | \overline{\boldsymbol{\kappa}}_{im} \right), if\ z_i = 1, \\ \mathbf{K}_{ij}, if\ z_i = 0. \end{cases} \tag{14}$$

The above formula integrates QIA decision making and Bayesian updates. If carrying out a QIA (i.e., $z_i = 1$ and a certain $x_{im} = 1$), the righthand side of Eq. (14) is equal to the posterior value of arc time and arc carbon emissions. If no QIA is carried out (i.e., $z_i = 0$ and each $x_{im} = 0$), the righthand side of Eq. (14) is equal to the original value.

3.3. Equivalent parameters between any two nodes in a GERT network

This part continues to develop the methodology when we need to calculate the equivalent Bayesian-updated parameters between any two nodes in a GERT network, by borrowing the ideas of moment-generating function (MGF) from the statistical field, as well as the transfer function (TF) and the Mason's gain formula both from the control system field.

3.3.1. Bayesian-updated bivariate moment-generating function

The classical bivariate MGF (BMGF) of two random variables is an alternative specification of their joint probability distribution. Since the two random variables (i.e., time and carbon emissions) in this study are Bayesian-updated parameters, the BMGF is defined as follows.

Definition 1. Let $M_{ij}^{\mathbf{H}}(\boldsymbol{\Lambda})$ be the BMGF of Bayesian-updated parameters vector $\mathbf{H}_{ij}$ (including time t_{ij} and carbon emissions c_{ij}). We call this BMGF a Bayesian-updated BMGF (BBMGF) which is formulated as

$$M_{ij}^{\mathbf{H}}(\mathbf{\Lambda}) = E\left(e^{\mathbf{\Lambda}^T \mathbf{H}_{ij}}\right), \tag{15}$$

where $\mathbf{\Lambda}$ is the vector of two dummy variables s_1 and s_2, i.e., $\mathbf{\Lambda} = \begin{pmatrix} s_1 \\ s_2 \end{pmatrix}$.

By referring to the proof on page 120 of Hogg and Craig (1978), we can rewrite BBMGF as

$$M_{ij}^{t,c}(s_1, s_2) = \begin{cases} e^{\mu_{ij1|im} s_1 + \mu_{ij2|im} s_2 + \frac{\sigma_{ij1|im}^2 s_1^2 + 2\rho_{ij|im}\sigma_{ij1|im}\sigma_{ij2|im} s_1 s_2 + \sigma_{ij2|im}^2 s_2^2}{2}}, if\ z_i = 1, \\ e^{\mu_{ij1} s_1 + \mu_{ij2} s_2 + \frac{\sigma_{ij1}^2 s_1^2 + 2\rho_{ij}\sigma_{ij1}\sigma_{ij2} s_1 s_2 + \sigma_{ij2}^2 s_2^2}{2}}, if\ z_i = 0; \end{cases} \tag{16}$$

where $\mu_{ij1|im}$ and $\sigma_{ij1|im}$ are respectively the mean and standard deviation of $\sum_m (x_{im} q_{ij} | \overline{\boldsymbol{\kappa}}_{\boldsymbol{im}})$; $\mu_{ij2|im}$ and $\sigma_{ij2|im}$ are respectively the mean and standard deviation of $\sum_m (x_{im} r_{ij} | \overline{\boldsymbol{\kappa}}_{\boldsymbol{im}})$; and $\rho_{ij|im}$ is the correlation between $\sum_m (x_{im} q_{ij} | \overline{\boldsymbol{\kappa}}_{\boldsymbol{im}})$ and $\sum_m (x_{im} r_{ij} | \overline{\boldsymbol{\kappa}}_{\boldsymbol{im}})$.

Define $M_{ij}^t(s_1)$ and $M_{ij}^c(s_2)$ as the Bayesian-updated univariate MGF (BUMGF) of time t_{ij} and carbon emissions c_{ij} respectively. By referring to the proofs on pages 111 and 120 of Hogg and Craig (1978), we can obtain Property 3.

Property 3. The relationships between the BBMGF and the BUMGFs are as follows:

$$M_{ij}^{t,c}(s_1, 0) = M_{ij}^t(s_1), \tag{17}$$

$$M_{ij}^{t,c}(0, s_2) = M_{ij}^c(s_2). \tag{18}$$

Then, according to an important characteristic of MGF, i.e., the first-order derivative of an MGF is equal to the first-order central moment (i.e., the mean) when the dummy variable is equal to zero, we can further obtain Property 4.

Property 4. The relationships between the BBMGF and the mean of Bayesian-updated time (respectively carbon emissions) are as follows:

$$\left.\frac{dM_{ij}^{t,c}(s_1,0)}{ds_1}\right|_{s_1=0} = E(t_{ij}), \tag{19}$$

$$\left.\frac{dM_{ij}^{t,c}(0,s_2)}{ds_2}\right|_{s_2=0} = E(c_{ij}). \tag{20}$$

3.3.2. Bayesian-updated multivariate transfer function

The classical TF of an arc in a GERT network integrates multiple parameters into a single parameter to decrease the complexity of the network. Since the arc parameters in this study are Bayesian-updated, the TF is defined as follows.

Definition 2. Let $W_{ij}^{t,c}(s_1, s_2)$ be the TF which integrates BBMGF $M_{ij}^{t,c}(s_1, s_2)$ and Bayesian-updated probability π_{ij} on arc (i, j). We call this the Bayesian-updated multivariate TF (BMTF) which is formulated as

$$W_{ij}^{t,c}(s_1, s_2) = \pi_{ij} \cdot M_{ij}^{t,c}(s_1, s_2). \tag{21}$$

Property 5. The relationship between the Bayesian-updated probability and the BMTF is

$$\pi_{ij} = W_{ij}^{t,c}(0,0). \tag{22}$$

By combining Eqs. (21) and (22), we can obtain

$$M_{ij}^{t,c}(s_1, s_2) = \frac{W_{ij}^{t,c}(s_1,s_2)}{W_{ij}^{t,c}(0,0)}. \tag{23}$$

By combining Eqs. (19), (20) and (23), we can obtain Property 6.

Property 6. The relationship between the mean of Bayesian-updated time (or carbon emissions) and the BMTF is as follows:

$$E(t_{ij}) = \frac{1}{W_{ij}^{t,c}(0,0)} \cdot \left.\frac{dW_{ij}^{t,c}(s_1,0)}{ds_1}\right|_{s_1=0}, \tag{24}$$

$$E(c_{ij}) = \frac{1}{W_{ij}^{t,c}(0,0)} \cdot \left.\frac{dW_{ij}^{t,c}(0,s_2)}{ds_2}\right|_{s_2=0}. \tag{25}$$

3.3.3. Mason's gain formula

After the formulations of BBMGF and BMTF, the Mason's gain formula, which is a mathematical tool in the signal flowgraph theory, is employed to calculate the equivalent BMTF (EBMTF) between any two nodes. Suppose that i and k are any two nodes, $i, k \in I$, $EW_{ik}^{t,c}(s_1, s_2)$ is the EBMTF between i and k in a GERT network. The Mason's gain formula is

presented as

$$EW_{ik}^{t,c}(s_1, s_2) = \frac{\sum_f P_{ikf} \cdot \Delta_{ikf}}{\Delta}, \tag{26}$$

where f is the serial number of a forward path (a forward path is a path from i to k and does not pass through any node more than once), P_{ikf} is the total gain (the total gain is the product of the BMTFs of all arcs in the fth forward path) of the fth forward path from i to k in a GERT network, Δ_{ikf} is the determinant of the sub-network formed by removing the fth forward path (from i to k) from a GERT network (the formula of the determinant of a sub-network is similar to the determinant of a GERT network shown below), Δ is the determinant of a GERT network and its expression is

$$\Delta = 1 + \sum_\eta \sum_l (-1)^\eta L_l^\eta, \tag{27}$$

where η is the order of the loop (a path that starts and ends at the same node, and does not pass through any other node more than once) in a GERT network, ηth-order loop refers to the set of η disconnected loops in a GERT network, l is the serial number of an ηth-order loop, and L_l^η is the total gain of the lth ηth-order loop in a GERT.

3.3.4. Equivalent Bayesian-updated parameters between any two nodes

In a GERT network with XOR nodes, any network structure is a combination of series, parallel and self-loop basic networks, in which the equivalent probability between any two nodes can be obtained by setting the dummy variable equal to zero in the equivalent TF, and the equivalent time/carbon emissions between any two nodes can be calculated by differentiating the equivalent TF with respect to the dummy variable and then setting the dummy variable equal to zero, which is proved on page 31 of Pritsker (1966). In addition, the Mason's gain formula does not change the network structure.

Then, similar to Pritsker (1966), Properties 5 and 6 can be extended to

$$\pi_{ik} = EW_{ik}^{t,c}(0,0), \tag{28}$$

$$E(t_{ik}) = \frac{1}{EW_{ik}^{t,c}(0,0)} \cdot \frac{dEW_{ik}^{t,c}(s_1,0)}{ds_1}\Big|_{s_1=0}, \tag{29}$$

$$E(c_{ik}) = \frac{1}{EW_{ik}^{t,c}(0,0)} \cdot \frac{dEW_{ik}^{t,c}(0,s_2)}{ds_2}\Big|_{s_2=0}. \tag{30}$$

where π_{ik} is the equivalent Bayesian-updated probability, $E(t_{ik})$ is the mean of equivalent Bayesian-updated time, and $E(c_{ik})$ is the mean of equivalent Bayesian-updated carbon emissions between any two nodes in a GERT network.

4. Multi-objective Model Formulation

This part builds a multi-objective model in the proposed three-echelon Bayesian-updated GERT networks to simultaneously pursue the total quality, total time and total carbon emissions.

4.1. Multiple objectives

We consider three objectives including maximizing total quality, minimizing total time and minimizing total carbon emissions from the perspective of producing a unit of bottled milk. The word "total" means the whole production steps from the beginning to the end. We regard the bottom-echelon GERT network in Fig. 2b as a big node numbered as Node 13 in terms of the middle-echelon network (Fig. 3a). The parameters outputted by Node 13 are $\pi_{13,7} = \pi_{57}\pi_{67}$, $t_{13,7} = max\{t_{57}, t_{67}\}$, $c_{13,7} = max\{c_{57}, c_{67}\}$.

Similarly, we regard the middle-echelon network as a big node numbered as Node 14 in terms of the top-echelon network (Fig. 3b). The parameters outputted by Node 14 are $\pi_{14,10} = \pi_{1,10}\pi_{13,10}$, $t_{14,10} = max\{E(t_{1,10}), E(t_{13,10})\}$, $c_{14,10} = max\{E(c_{1,10}), E(c_{13,10})\}$.

(a) Middle-echelon Network (b) Top-echelon network

Fig. 3 The network structure in different echelon

Then, we consider the top-echelon network (i.e., the whole network). Arcs (9,10) and

(14,10) need to emerge into one arc, which is equal to updating the parameters of arc (9,10) by arc (14,10) in a closed-loop network. Note that the parameters of arc (9,10) are affected not only by arc (14,10) but also by itself, due to the feedback arcs (10,9) and (11,9), and the self-loop arc (9,9). Therefore, we propose an approximation method detailed as follows.

Step 1. Define a generation vector denoted as $\langle a_1, a_2 \rangle$ in which a_1 ($a_1 = 0,1,2,\cdots$) means the generation updated by arc (14,10), and a_2 ($a_2 = 0,1,2,\cdots$) means the generation updated by feedback and self-loop arcs. Let $\langle a_1, a_2 \rangle$ be a temporary superscript for parameters of arc (9,10), i.e., $\left(\pi_{9,10}^{\langle a_1,a_2 \rangle}, t_{9,10}^{\langle a_1,a_2 \rangle}, c_{9,10}^{\langle a_1,a_2 \rangle}\right)$.

Step 2. Let the Bayesian-updated probability, time, and carbon emissions of arc (9,10) resulting from QIA decision making be the initial generation, denoted as $\left(\pi_{9,10}^{\langle 0,0 \rangle}, t_{9,10}^{\langle 0,0 \rangle}, c_{9,10}^{\langle 0,0 \rangle}\right) = \left(\pi_{9,10}, t_{9,10}, c_{9,10}\right)$.

Step 3. Update the present generation. We will obtain two individuals of the next generation.

Step 3.1. Update the present generation by arc (14,10). We will obtain the first individual whose parameters are calculated by $\pi_{9,10}^{\langle a_1+1,a_2 \rangle} = \pi_{9,10}^{\langle a_1,a_2 \rangle}\pi_{14,10}$, $t_{9,10}^{\langle a_1+1,a_2 \rangle} = max\left\{t_{9,10}^{\langle a_1,a_2 \rangle}, t_{14,10}\right\}$, and $c_{9,10}^{\langle a_1+1,a_2 \rangle} = max\left\{c_{9,10}^{\langle a_1,a_2 \rangle}, c_{14,10}\right\}$.

Step 3.2. Update the first individual of the next generation by feedback and self-loop arcs. By using the methodology in Section 3.3, we will obtain the second individual $\left(\pi_{9,10}^{\langle a_1+1,a_2+1 \rangle}, t_{9,10}^{\langle a_1+1,a_2+1 \rangle}, c_{9,10}^{\langle a_1+1,a_2+1 \rangle}\right)$.

Step 4. Evaluate the gap between two individuals of the same generation, and decide whether to continue with the next iteration. Let η be a threshold. If the gap satisfies

$$max\left\{\frac{\left|\pi_{9,10}^{\langle a_1+1,a_2+1 \rangle} - \pi_{9,10}^{\langle a_1+1,a_2 \rangle}\right|}{\pi_{9,10}^{\langle a_1+1,a_2 \rangle}}, \frac{\left|t_{9,10}^{\langle a_1+1,a_2+1 \rangle} - t_{9,10}^{\langle a_1+1,a_2 \rangle}\right|}{t_{9,10}^{\langle a_1+1,a_2 \rangle}}, \frac{\left|t_{9,10}^{\langle a_1+1,a_2+1 \rangle} - t_{9,10}^{\langle a_1+1,a_2 \rangle}\right|}{t_{9,10}^{\langle a_1+1,a_2 \rangle}}\right\} \leq \eta,$$

then stop, and rewrite $\left(\pi_{9,10}, t_{9,10}, c_{9,10}\right) = \left(\pi_{9,10}^{\langle a_1+1,a_2+1 \rangle}, t_{9,10}^{\langle a_1+1,a_2+1 \rangle}, c_{9,10}^{\langle a_1+1,a_2+1 \rangle}\right)$. Otherwise, rewrite $a_1 = a_1 + 1, a_2 = a_2 + 1$, and repeat Step 3. □

Finally, we develop the three objective functions as follows:

$$G_1 = max\, \pi_{9,12}, \tag{31}$$

$$G_2 = min\, E\left(t_{9,12}\right), \tag{32}$$

$$G_3 = min\, E\left(c_{9,12}\right). \tag{33}$$

4.2. A customized algorithm

The above model appears as a multi-objective nonlinear stochastic dynamic programming model. Solving such a model with a large-scale numerical example by common mathematical software is time-consuming and sometimes intractable. In order to accelerate the search for the feasible non-dominated solutions (NDSs) and plot Pareto front more quickly, we employ a metaheuristic called customized MOPSO (CMOPSO) which integrates the classical MOPSO, a voting strategy, the approximation method for developing objective functions, and the Bayesian-updated GERT.

4.2.1. Decision-variable coding by a voting strategy

A classical MOPSO involves an iterative program in which a particle u $(u = 1,2,\cdots,U)$ moves in the multi-dimensional space during each iteration w with an iteration-dependent position X_u^w and velocity V_u^w. Each particle always searches and updates its individual best position P_u^w and global best position P_{best}^w (Moslemi and Zandieh, 2011; Govindan et al., 2014; Tabrizi et al., 2018). X_u^w, V_u^w, P_u^w and P_{best}^w in this study are all $(I + \sum_i \Omega_i) \times 1$ vectors, because a particle embraces the information of all decision variables. However, the two types of decision variables (i.e., location variables and allocation variables) are both binary variables which interrelate with each other by Eq. (1). Therefore, the immediate use of binary coding for both types of variables will lead to too many infeasible solutions. In this case, we propose a voting strategy detailed as follows.

(1) Particle initialization

First, a binary value of 0 or 1 is randomly provided to each node, which indicates whether a node is chosen or not to carry out a QIA. Then, each QIA candidate of a chosen node is randomly provided a vote (a nonnegative real number). The candidate which possesses the most votes will win the selection, that is, this QIA candidate will be carried out in the node which is chosen beforehand. Using this strategy, Eq. (1) is equivalent to

$$x_{im} = \begin{cases} z_i, \ if \ v_{im} = \max_m v_{im}, \\ 0, \ if \ v_{im} \neq \max_m v_{im}; \end{cases} \tag{34}$$

where v_{im} represents the vote received by QIA ω_{im}.

Hence, the position vector of a particle falls into two sub-vectors (i.e., the discrete sub-vector $\mathrm{X}_{\mathrm{u1}}^{\mathrm{w}}$ and the continuous sub-vector X_{u2}^{w}), and is shown as

$$X_u^w = \begin{bmatrix} X_{u1}^w \\ X_{u2}^w \end{bmatrix}, \tag{35}$$

where

$$X_{u1}^w = [z_1, \cdots, z_I]^T, \tag{36}$$

$$X_{u2}^w = [v_{11}, \cdots, v_{1\Omega_1}, v_{21}, \cdots, v_{2\Omega_2}, \cdots, v_{I1}, \cdots, v_{I\Omega_I}]^T. \tag{37}$$

Similarly, the velocity vector of a particle is also divided into two sub-vectors (i.e., the discrete sub-vector $\mathrm{V}_{u1}^{\mathrm{w}}$ and the continuous sub-vector V_{u2}^{w}), and is shown as

$$V_u^w = \begin{bmatrix} V_{u1}^w \\ V_{u2}^w \end{bmatrix}. \tag{38}$$

(2) Particle update

Without loss of generality, the velocity of a particle is updated by

$$V_u^{w+1} = \varpi V_u^w + c_1 R(P_u^w - X_u^w) + c_2 R(P_{best}^w - X_u^w), \tag{39}$$

where R is a number randomly generated from the range between 0 and 1, ϖ is the inertia weight with a damping rate related to iteration time, and c_1 and c_2 are the learning factors.

Different from the update of the velocity, the update of the position depends on the sub-vector types of the position vector. In terms of discrete sub-vector, the Sigmoid function is employed to transform the discrete sub-vector of the updated velocity into a position-related probability φ_{u1}^{w+1} which is formulated as

$$\varphi_{u1}^{w+1} = \frac{1}{1+e^{-V_{u1}^{w+1}}}. \tag{40}$$

Then, the discrete sub-vector of the position is updated by

$$X_{u1}^{w+1} = \begin{cases} 1, if\ R \le \varphi_{u1}^{w+1}, \\ 0, otherwise. \end{cases} \tag{41}$$

In terms of continuous sub-vector, the updated position is

$$X_{u2}^{w+1} = X_{u2}^{w} + V_{u2}^{w+1}. \tag{42}$$

4.2.2. Algorithm procedure

Fig. 4 shows the details of how the CMOPSO integrates the classical MOPSO, the voting strategy, the approximation method, and the Bayesian-updated GERT.

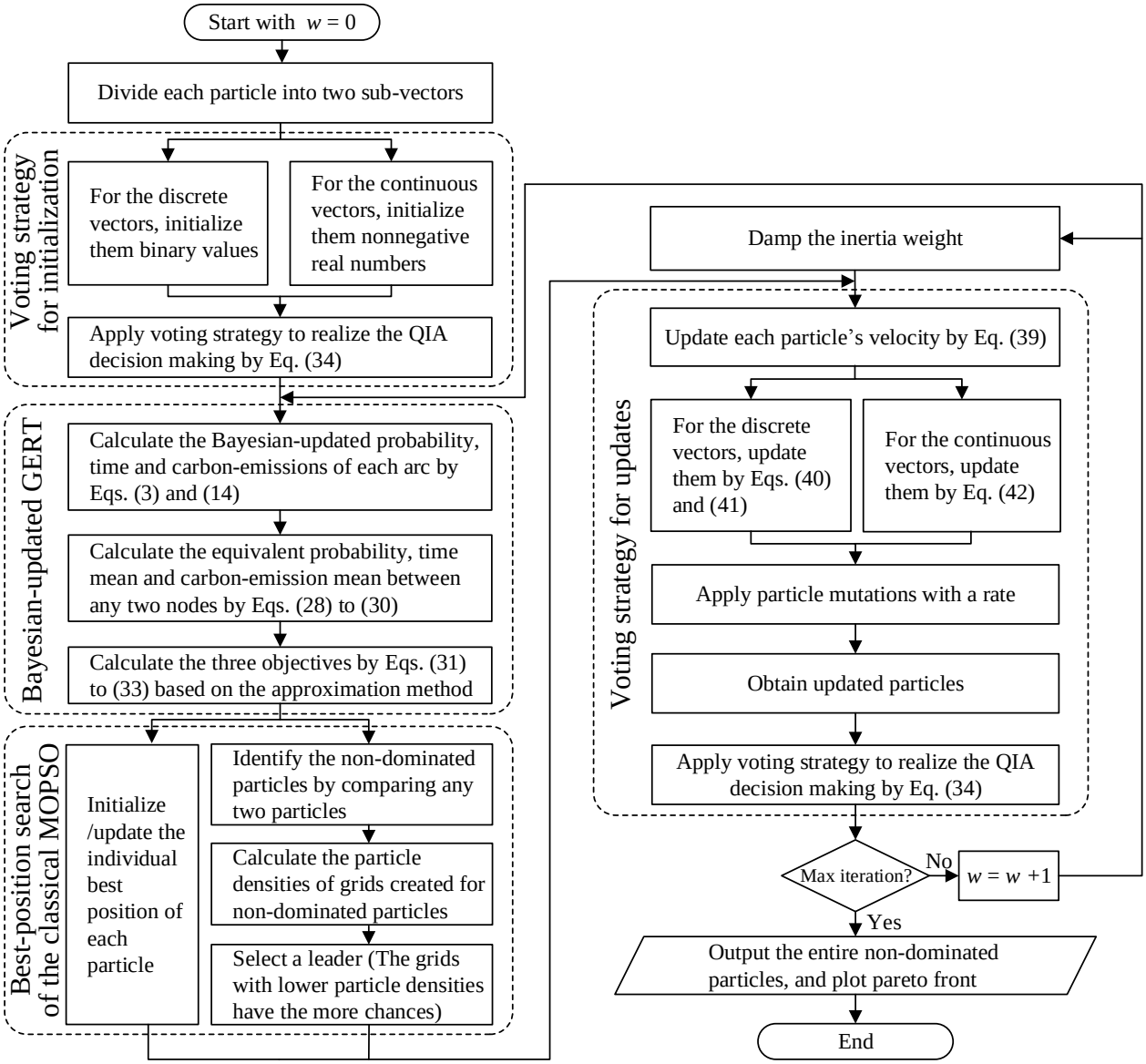

Fig.4 The procedure of the CMOPSO

5. Case Study

5.1. Case description

The model and approach in this study are applied to a real case based on our on-the-spot investigation. A famous dairy manufacturing firm called Beingmate has mature and self-owned production lines, and accumulated plenty of dairy-production experience and historical data. Its production steps of bottled milk, shown beforehand as three-echelon GERT networks in Fig. 2b, are comparatively fixed but, the efficacy, the efficiency, and the environmental friendliness of the

network arcs are to be further optimized. Table 2 lists the possible QIAs and Table 3 shows their attributes. The DM of the firm tries to carry out QIAs to update the original attributes of arcs. As listed in Table 4, these original attributes of arcs show the status quo of the bottled milk production lines. A QIA can be not only a single mechanized operation or food safety inspection technology, but also arbitrary combinations of them. Furthermore, a QIA will affect the values of arc parameters, whose extents are recorded by relational databases shown in Table 5. These databases are very valuable and set up by the cooperation of Beingmate and us. Presently, Beingmate faces the problem of QIA decision making to put forward sustainable quality management plans.In addition, let the maximum iterations be 300, the particle population size be 200, the NDS population size be 150, the inertia weight be 1 with a damping rate 0.99, and two learning factors be both 1.5, and the gap threshold in the approximation method be 0.01. The CMOPSO is coded by MATLAB R2017b on a 3.4 GHz laptop with 8 GB of RAM.

5.2. Tradeoffs of multiple objectives

After running for 359 seconds, the Pareto front is achieved (Fig. 5a). Due to the existence of the three objectives, the Pareto front emerges as a curved surface with an inclined shape. We call it "surface of Pareto front" (SPF) and the star-shaped points composing the SPF "global NDSs" (GNDSs). The GNDSs hold the non-dominated locations and are derived from the particles who are moving towards point A (the ideal point for all three objectives). Therefore, no particles exist below the SPF.

Table 2 The QIA candidates in each node

QIAs \ Nodes	1	2	3	4	5	6	7	8	9	10	11
QIA1	①Detecting forage	①Using milk purifier	①Using UHT machines	①Filling by machines	①Sensory tests	①Testing preservative	①Sterilizing by machines	①Filling by machines	①Filling by machines	①Using UHT machines	①Low-temp transportation
QIA2	②Training feeders	②Alcohol tests	②Microbial tests	②Testing lead tank	②Microbial tests	②Testing pesticide	②Microbial tests	②Microbial tests	②Sterilizing the bottles	②Microbial tests	②Low-temp storing
QIA3	③Testing antibiotics	③Using homogenizer	③Training operators	③Training operators	③Testing mineral content	③Fresh-keeping packaging	③Training operators	③Low-temp filling	③Low-temp filling	③Training operators	③Protective packaging
QIA4	④Milking by machines	④Low-temp storing	④Cleaning the plant	④Low-temp filling	④Low-temp storing	④Low-temp storing	④Sterilizing the plant	④Improving the recycling	④Improving the recycling	④Improving the recycling	④Improving the recycling
QIA5	①+②	①+②	①+②	①+②	①+②	①+②	①+②	①+②	①+②	①+②	①+②
QIA6	①+③	①+③	①+③	①+③	①+③	①+③	①+③	①+③	①+③	①+③	①+③
QIA7	①+④	①+④	①+④	①+④	①+④	①+④	①+④	①+④	①+④	①+④	①+④
QIA8	②+③	②+③	②+③	②+③	②+③	②+③	②+③	②+③	②+③	②+③	②+③
QIA9	②+④	②+④	②+④	②+④	②+④	②+④	②+④	②+④	②+④	②+④	②+④
QIA10	③+④	③+④	③+④	③+④	③+④	③+④	③+④	③+④	③+④	③+④	③+④
QIA11	①+②+③	①+②+③	①+②+③	①+②+③	①+②+③	①+②+③	①+②+③	①+②+③	①+②+③	①+②+③	①+②+③
QIA12	①+②+④	①+②+④	①+②+④	①+②+④	①+②+④	①+②+④	①+②+④	①+②+④	①+②+④	①+②+④	①+②+④
QIA13	①+③+④	①+③+④	①+③+④	①+③+④	①+③+④	①+③+④	①+③+④	①+③+④	①+③+④	①+③+④	①+③+④
QIA14	②+③+④	②+③+④	②+③+④	②+③+④	②+③+④	②+③+④	②+③+④	②+③+④	②+③+④	②+③+④	②+③+④
QIA15	①+②+③+④	①+②+③+④	①+②+③+④	①+②+③+④	①+②+③+④	①+②+③+④	①+②+③+④	①+②+③+④	①+②+③+④	①+②+③+④	①+②+③+④

Table 3 The attributes of the QIA candidates in each node

QIAs \ Nodes	1	2	3	4	5	6	7	8	9	10	11
QIA1	300,50,0.5 6.54,1.09	300,50,0.4 13.08,2.18	5,0.83,0.45 10.9,1.82	5,0.83,0.6 0.22,0.04	200,33.33,0.7 4.36,0.73	120,20,0.55 2.62,0.44	60,10,0.25 26.16,4.36	5,0.83,0.3 0.22,0.04	5,0.83,0.2 0.22,0.04	5,0.83,0.6 10.9,1.82	600,100,0.35 100,16.67
QIA2	600,100,0.6 1,0.17	180,30,0.7 0.39,0.07	300,50,0.7 6.54,1.09	60,10,0.4 1.31,0.22	300,50,0.55 6.54,1.09	60,10,0.3 1.31,0.22	300,50,0.5 6.54,1.09	300,50,0.55 6.54,1.09	60,10,0.4 26.16,4.36	300,50,0.55 6.54,1.09	100,17,0.3 13.63,2.27
QIA3	60,10,0.55 1.31,0.22	400,67,0.65 17.44,2.91	500,83,0.35 1,0.17	500,83,0.8 1,0.17	400,67,0.5 8.72,1.45	90,15,0.55 2,0.33	500,83,0.45 1,0.17	120,20,0.35 16.35,2.73	90,15,0.6 12.26,2.04	500,83,0.7 1,0.17	90,15,0.5 2,0.33
QIA4	5,0.83,0.3 0.55,0.09	900,150,0.7 122,20.33	600,100,0.5 6.81,1.14	60,10,0.3 8.13,1.36	60,10,0.3 8.13,1.36	70,12,0.65 9.5,1.58	600,100,0.8 6.81,1.14	120,20,0.45 3.92,0.65	90,15,0.3 2.94,0.49	80,13,0.4 2.62,0.44	70,11,0.3 2.29,0.38
QIA5	900,150,0.55 7.54,1.26	480,80,0.3 13.47,2.25	305,51,0.55 17.44,2.91	65,11,0.35 1.53,0.26	500,83,0.35 10.9,1.82	180,30,0.6 3.93,0.66	360,60,0.35 32.7,5.45	305,51,0.5 6.76,1.13	65,11,0.55 26.38,4.4	305,51,0.3 17.44,2.91	700,117,0.45 113.63,18.94
QIA6	360,60,0.4 7.85,1.31	700,117,075 30.52,5.09	505,84,0.75 11.9,1.98	505,84,0.5 1.22,0.2	600,100,0.6 13.08,2.18	210,35,0.7 4.62,0.77	560,93,0.5 27.16,4.53	125,21,0.45 16.57,2.76	95,16,0.5 12.48,2.08	505,84,0.6 11.9,1.98	690,115,0.7 102,17
QIA7	305,51,0.45 7.09,1.18	1200,200,0.65 135.08,22.51	605,101,0.6 17.71,2.95	65,11,0.55 8.35,1.39	260,43,0.3 12.49,2.08	190,32,0.5 12.12,2.02	660,110,0.65 32.97,5.5	125,21,0.7 4.14,0.69	95,16,0.3 3.16,0.53	85,14,0.5 13.52,2.25	670,112,0.6 102.29,17.05
QIA8	660,110,0.6 2.31,0.39	580,97,0.5 17.83,2.97	800,133,0.5 7.54,1.26	560,93,0.8 2.31,0.39	700,117,0.75 15.26,2.54	150,25,0.45 3.31,0.55	800,133,0.8 7.54,1.26	420,70,0.5 22.89,3.82	150,25,0.4 38.42,6.4	800,133,0.75 7.54,1.26	190,32,0.5 15.63,2.61
QIA9	605,101,0.5 1.55,0.26	1080,180,0.8 122.39,20.4	900,150,0.35 13.35,2.23	120,20,0.65 9.44,1.57	360,60,0.7 14.67,2.45	130,22,0.3 10.81,1.8	900,150,0.35 13.35,2.23	420,70,0.75 10.46,1.74	150,25,0.6 29.1,4.85	380,63,0.3 9.16,1.53	170,28,0.8 15.92,2.65
QIA10	65,11,0.8 1.86,0.31	1300,217,0.6 139.44,23.24	1100,183,0.4 7.81,1.3	560,93,0.85 9.13,1.52	460,77,0.55 16.85,2.81	160,27,0.8 11.5,1.92	1100,183,0.5 7.81,1.3	240,40,0.4 20.27,3.38	180,30,0.65 15.2,2.53	580,97,0.7 3.62,0.6	160,27,0.85 4.29,0.72
QIA11	960,160,0.6 8.85,1.48	880,147,0.65 30.91,5.15	805,134,0.8 18.44,3.07	565,94,0.7 2.53,0.42	900,150,0.5 19.62,3.27	270,45,0.45 5.93,0.99	860,143,0.75 33.7,5.62	425,71,0.8 23.11,3.85	155,26,0.45 38.64,6.44	805,134,0.5 18.44,3.07	790,132,0.6 115.63,19.27
QIA12	905,151,0.4 8.09,1.35	1380,230,0.7 135.47,22.58	905,151,0.7 24.25,4.04	125,21,0.5 9.66,1.61	560,93,0.75 19.03,3.17	250,42,0.5 13.43,2.24	960,160,0.55 39.51,6.59	425,71,0.65 10.68,1.78	155,26,0.8 29.32,4.89	385,64,0.85 20.06,3.34	770,128,0.5 115.92,19.32
QIA13	365,61,0.85 8.4,1.4	1600,267,0.8 152.52,25.42	1105,184,0.85 18.71,3.12	565,94,0.7 9.35,1.56	660,110,0.4 21.21,3.54	280,47,0.65 14.12,2.35	1160,193,0.85 33.97,5.66	245,41,0.55 20.49,3.42	185,31,0.7 15.42,2.57	585,98,0.5 14.52,2.42	760,127,0.75 104.29,17.38
QIA14	665,111,0.7 2.86,0.48	1480,247,0.85 139.83,23.31	1400,233,0.75 14.35,2.39	620,103,0.75 10.44,1.74	760,127,0.8 23.39,3.9	220,37,0.5 12.81,2.14	1400,233,0.6 14.35,2.39	540,90,0.5 26.81,4.47	240,40,0.4 41.36,6.89	880,147,0.4 10.16,1.69	260,43,0.8 17.92,2.99
QIA15	965,161,0.8 9.4,1.57	1780,297,0.6 152.91,25.49	1405,234,0.45 25.25,4.21	625,104,0.5 10.66,1.78	960,160,0.5 27.75,4.63	340,57,0.8 15.43,2.57	1460,243,0.75 40.51,6.75	545,91,0.7 27.03,4.51	245,41,0.85 41.58,6.93	885,148,0.6 21.06,3.51	860,143,0.7 117.92,19.65

Note: each cell sequentially lists $\theta_{im1}, \tau_{im1}, \nu_{im}, \theta_{im2}, \tau_{im2}$.

Table 4 The attributes of the arcs

Arcs	1,2	1,0	2,3	2,0	3,4	3,0	4,10	4,0	5,7	5,0	6,7	6,0	7,8	7,0	8,8	8,10	8,0	9,9	9,10	9,0	10,9	10,1	10,1	10,0	11,9	11,1	11,0
α_{ij}	19	3	23	3	26	4	25	3	25	2	22	3	34	4	18	29	4	19	25	3	9	18	13	3	9	20	3
$\mu_{ij1}(s)$	30	/	900	/	1000	/	60	/	60	/	70	/	720	/	120	60	/	90	60	/	90	900	120	/	80	100	/
$\sigma_{ij1}(s)$	5	/	150	/	160	/	10	/	10	/	12	/	120	/	20	10	/	15	10	/	15	150	20	/	13	16	/
$\mu_{ij2}(g)$	0.06	/	30	/	33	/	0.12	/	2.62	/	3	/	24	/	2.62	0.12	/	2	0.12	/	2	30	1.6	/	1.8	1.2	/
$\sigma_{ij2}(g)$	0.01	/	5	/	5.5	/	0.02	/	0.44	/	0.5	/	4	/	0.44	0.02	/	0.33	0.02	/	0.33	5	0.25	/	0.3	0.2	/
ρ_{ij}	0.15	/	0.62	/	0.65	/	0.18	/	0.76	/	0.78	/	0.63	/	0.45	0.19	/	0.42	0.13	/	0.48	0.64	0.31	/	0.46	0.35	/

Table 5 The relationships between the QIA candidates and the arcs

QIAs	1,2	2,3	3,4	4,10	5,7	6,7	7,8	8,8	8,10	9,9	9,10	10,9	10,11	10,12	11,9	11,12
QIA1	0.91,33 0.99,0.73 0.41,1.3	0.25,33 0.30,1.45 0.77,1.3	0.01,1 0.25,1.21 0.93,1.9	1.00,1 0.65,0.02 0.75,1.3	0.77,22 0.62,0.48 0.45,1.1	0.63,13 0.47,0.29 0.42,1.1	0.08,7 0.52,2.91 0.92,1.8	0.08,1 0.08,0.02 0.69,1.1	1.00,1 0.65,0.02 0.77,1.2	0.14,1 0.10,0.02 0.65,1.1	1.00,1 0.65,0.02 0.72,1.2	0.05,1 0.84,1.09 0.86,1.0	0.01,1 0.27,1.21 0.96,1.0	0.04,1 0.87,1.15 0.77,1.8	0.88,60 0.98,10 0.81,1.1	0.86,67 0.99,11.1 0.90,1.7
QIA2	0.95,67 0.94,0.11 0.19,1.1	0.17,20 0.01,0.04 0.13,1.1	0.23,33 0.17,0.73 0.46,1.3	0.50,7 0.92,0.15 0.43,1.2	0.83,33 0.71,0.73 0.45,1.3	0.46,7 0.30,0.15 0.44,1.2	0.29,33 0.21,0.73 0.49,1.3	0.71,30 0.71,0.65 0.41,1	0.83,33 0.98,0.73 0.45,1.3	0.40,6 0.93,2.62 0.85,1.0	0.50,7 1.00,2.91 0.95,1.6	0.77,30 0.77,0.65 0.39,1.0	0.25,33 0.18,0.73 0.43,1.3	0.71,32 0.80,0.69 0.35,1.3	0.56,10 0.88,1.36 0.78,1.1	0.50,11 0.92,1.51 0.86,1.6
QIA3	0.67.7 0.96,0.15 0.44,1.2	0.31.44 0.37,1.94 0.73,1.5	0.33.56 0.03,0.11 0.14,1.1	0.89.56 0.89,0.11 0.15,1.1	0.87.44 0.77,0.97 0.42,1.2	0.56.10 0.40,1.22 0.48,1.3	0.41.56 0.04, 0.11 0.12,1.1	0.50.12 0.86,1.64 0.78,1.1	0.67.13 0.99,1.82 0.87,1.9	0.50.9 0.86,1.23 0.78,1.2	0.60.10 0.99,1.36 0.87,1.7	0.85.50 0.33,0.10 0.10,1.1	0.36.56 0.03,0.11 0.11,1.1	0.81.53 0.38,0.11 0.09,1.1	0.53.9 0.53,0.20 0.45,1.2	0.47.10 0.63,0.22 0.50,1.2
QIA4	1.00.1 0.90,0.06 0.71,1.9	0.50.100 0.8,13.56 0.90,1.7	0.38.67 0.17,0.76 0.34,1.2	0.50.7 0.99,0.90 0.82,1.8	0.50.7 0.76,0.90 0.88,1.8	0.50.8 0.76,1.06 0.86,1.8	0.45.67 0.22,0.76 0.31,1.2	0.50.12 0.60,0.39 0.63,1.3	0.67.13 0.97,0.44 0.70,1.0	0.50.9 0.60,0.29 0.56,1.4	0.60.10 0.96,0.33 0.62,1.0	0.47.8 0.57,0.26 0.58,1.4	0.08.9 0.08,0.29 0.64,1.0	0.40.8 0.62,0.28 0.52,1.0	0.47.7 0.56,0.23 0.56,1.4	0.41.8 0.66,0.25 0.62,1.0
QIA5	0.97.100 0.99,0.84 0.12,1.4	0.35.53 0.31,1.50 0.48,1.4	0.23.34 0.35,1.94 0.70,2.2	1.00.7 0.93,0.17 0.44,1.5	0.89.56 0.81,1.21 0.49,1.4	0.72.20 0.57,0.44 0.45,1.3	0.33.40 0.58,3.63 0.74,2.1	0.84.31 0.72,0.68 0.36,1.1	1.00.34 0.98,0.75 0.40,1.5	0.68.7 0.93,2.64 0.87,1.1	1.00.7 1.00,2.93 0.96,1.8	0.77.31 0.90,1.74 0.63,1.0	0.25.34 0.37,1.94 0.70,1.3	0.72.32 0.92,1.84 0.56,2.1	0.90.70 0.98,11.4 0.75,1.2	0.88.78 0.99,12.6 0.83,2.3
QIA6	0.92.40 0.99,0.87 0.44,1.5	0.44.78 0.50,3.39 0.71,1.8	0.34.56 0.27,1.32 0.45,2	1.00.56 0.91,0.14 0.11,1.4	0.91.67 0.83,1.45 0.49,1.3	0.75.23 0.61,0.51 0.49,1.4	0.44.62 0.53,3.02 0.77,1.9	0.68.13 0.86,1.66 0.74,1.2	1.00.14 0.99,1.84 0.82,2.1	0.76.10 0.86,1.25 0.76,1.3	1.00.11 0.99,1.39 0.85,1.9	0.85.51 0.86,1.19 0.39,1.1	0.36.56 0.28,1.32 0.44,1.1	0.81.53 0.88,1.25 0.35,1.9	0.90.69 0.98,10.2 0.80,1.3	0.87.77 0.99,11.3 0.89,1.9
QIA7	1.00.34 0.99,0.79 0.43,2.2	0.57.133 0.82,15.0 0.87.2	0.38.67 0.35,1.97 0.46,2.1	1.00.7 0.99,0.93 0.82,2.1	0.81.29 0.83,1.39 0.77,1.9	0.73.21 0.80,1.35 0.78,1.9	0.48.73 0.58,3.66 0.78,2	0.68.13 0.61,0.41 0.58,1.4	1.00.14 0.97,0.46 0.65,1.2	0.76.10 0.61,0.32 0.57,1.5	1.00.11 0.96,0.35 0.63,1.2	0.49.9 0.87,1.35 0.75,1.4	0.09.9 0.31,1.50 0.83,1.0	0.41.9 0.89,1.42 0.66,1.8	0.89.67 0.98,10.2 0.73,1.5	0.87.74 0.99,11.4 0.81,1.7
QIA8	0.96.73 0.97,0.26 0.16,1.3	0.39.64 0.37,1.98 0.45,1.6	0.44.89 0.19,0.84 0.10,1.4	0.90.62 0.95,0.26 0.18,1.3	0.92.78 0.85,1.70 0.44,1.5	0.68.17 0.52,0.37 0.42,1.5	0.53.89 0.24,0.84 0.19,1.4	0.78.42 0.90,2.29 0.70,1.1	0.88.47 0.99,2.54 0.78,2.2	0.63.15 0.95,3.84 0.85,1.2	0.71.17 1.00,4.27 0.95,2.3	0.90.80 0.79,0.75 0.17,1.1	0.47.89 0.20,0.84 0.19,1.4	0.87.84 0.82,0.79 0.15,1.4	0.70.19 0.90,1.56 0.69,1.3	0.66.21 0.93,1.74 0.76,1.8
QIA9	1.00.67 0.96,0.17 0.16,2	0.55.120 0.80,13.6 0.83,1.8	0.47.100 0.29,1.48 0.34,1.5	0.67.13 0.99,1.05 0.70,2	0.86.40 0.85,1.63 0.62,2.1	0.65.14 0.78,1.20 0.80,2	0.56.100 0.36,1.48 0.30,1.5	0.78.42 0.80,1.05 0.39,1.3	0.88.47 0.99,1.16 0.44,1.3	0.63.15 0.94,2.91 0.72,1.4	0.71,17 1.00,3.23 0.80,1.6	0.81,38 0.82,0.92 0.37,1.4	0.30,42 0.23,1.02 0.41,1.3	0.76.40 0.85,0.96 0.33,1.3	0.68.17 0.90,1.59 0.68,1.5	0.63.19 0.93,1.77 0.76,1.6
QIA10	1.00.7 0.97,0.21 0.49,2.1	0.59.144 0.82,15.5 0.78,2.2	0.52.122 0.19,0.87 0.19,1.3	0.90 .62 0.99,1.01 0.33,1.9	0.88.51 0.87,1.87 0.68,2	0.70.18 0.79,1.28 0.72,2.1	0.60.122 0.25,0.87 0.20,1.3	0.67.24 0.89,2.03 0.66,1.4	0.80.27 0.99,2.25 0.74,1.9	0.67.18 0.88,1.52 0.66,1.6	0.75.20 0.99,1.69 0.74,1.7	0.87.58 0.64,0.36 0.10,1.5	0.39.64 0.11,0.40 0.11,1.1	0.83.61 0.69,0.38 0.09,1.1	0.67.16 0.70,0.43 0.43,1.6	0.62.18 0.78,0.48 0.47,1.2
QIA11	0.97.107 0.99,0.98 0.13,1.6	0.49.98 0.51,3.43 0.62,1.9	0.45.89 0.36,2.05 0.41,2.5	1.00.63 0.95,0.28 0.16,1.6	0.94.100 0.88,2.18 0.43,1.6	0.79.30 0.66,0.66 0.47,1.6	0.54.96 0.58,3.74 0.63,2.2	0.88.43 0.90,2.31 0.64,1.2	1.00.47 0.99,2.57 0.71,2.4	0.84.16 0.95,3.86 0.85,1.3	1.00.17 1.00,4.29 0.94,2.5	0.90.81 0.90,1.84 0.41,1.1	0.47.89 0.38,2.05 0.46,1.4	0.87.85 0.92,1.94 0.37,2.2	0.91.79 0.98,11.6 0.81,1.4	0.89.88 0.99,12.9 0.90,2.5
QIA12	1.00.101 0.99,0.90 0.11,2.3	0.61.153 0.82,15.1 0.76,2.1	0.48.101 0.42,2.69 0.41,2.4	1.00.14 0.99,1.07 0.77,2.3	0.90.62 0.88,2.11 0.63,2.2	0.78.28 0.82,1.49 0.71,2.1	0.57.107 0.62,4.39 0.70,2.3	0.88.43 0.80,1.07 0.40,1.4	1.00.47 0.99,1.19 0.45,1.5	0.84.16 0.94,2.93 0.75,1.5	1.00.17 1.00,3.26 0.84,1.8	0.81.39 0.91,2.01 0.70,1.4	0.30.43 0.40,2.23 0.78,1.3	0.76.41 0.93,2.11 0.62.2.1	0.91.77 0.98,11.6 0.80,1.6	0.89.86 0.99,12.9 0.88,2.3
QIA13	1.00.41 0.99,0.93 0.44,2.4	0.64.178 0.84,17 0.72,2.5	0.52.123 0.36,2.08 0.31,2.2	1.00.63 0.99,1.04 0.37,2.2	0.92.73 0.89,2.36 0.61,2.1	0.80.31 0.82,1.57 0.78,2.2	0.62.129 0.59,3.77 0.49,2.1	0.80.25 0.89,2.05 0.70,1.5	1.00.27 0.99,2.28 0.78,2.1	0.86.19 0.89,1.54 0.71,1.7	1.00.21 0.99,1.71 0.78,1.9	0.87.59 0.88,1.45 0.43,1.5	0.39.65 0.33,1.61 0.48,1.1	0.83.62 0.90,1.53 0.38,1.9	0.90.76 0.98,10.4 0.75,1.7	0.88.84 0.99,11.6 0.83,1.9
QIA14	1.00.74 0.98,0.32 0.11,2.2	0.62.164 0.82,15.5 0.72,2.3	0.58.156 0.30,1.59 0.37,1.6	0.91.69 0.99,1.16 0.33,2.1	0.93.84 0.90,2.60 0.43,2.3	0.76.24 0.81,1.42 0.74,2.3	0.66.156 0.37,1.59 0.31,1.6	0.82 .54 0.91,2.68 0.68,1.4	0.90.60 1.00,2.98 0.75,2.2	0.73.24 0.95,4.14 0.75,1.6	0.80.27 1.00,4.60 0.83,2.3	0.91.88 0.84,1.02 0.32,1.5	0.49.98 0.25,1.13 0.35,1.4	0.88.93 0.86,1.07 0.28,1.4	0.76.26 0.91,1.79 0.71,1.7	0.72.29 0.94,1.99 0.78,1.8
QIA15	1.00.107 0.99,1.04 0.20,2.5	0.66.198 0.84,17 0.79,2.6	0.58.156 0.43,2.81 0.36,2.5	1.00.69 0.99,1.18 0.39,2.4	0.94.107 0.91,3.08 0.43,2.4	0.83.38 0.84,1.71 0.77,2.4	0.67.162 0.63,4.50 0.41,2.4	0.90.55 0.91,2.70 0.70,1.5	1.00.61 1.00,3.00 0.78,2.4	0.89.25 0.95,4.16 0.75,1.7	1.00.27 1.00,4.62 0.83,2.5	0.91,89 0.91,2.11 0.38,1.5	0.50.98 0.41,2.34 0.43,1.4	0.88.93 0.93,2.22 0.34 ,2.2	0.91.86 0.98,11.8 0.76,1.8	0.90.96 0.99,13.1 0.85,2.5

Note: each cell sequentially lists $\theta_{im1|ij}, \tau_{im1|ij}, \theta_{im2|ij}, \tau_{im2|ij}, \nu_{im|ij}, \lambda_{imj}$.

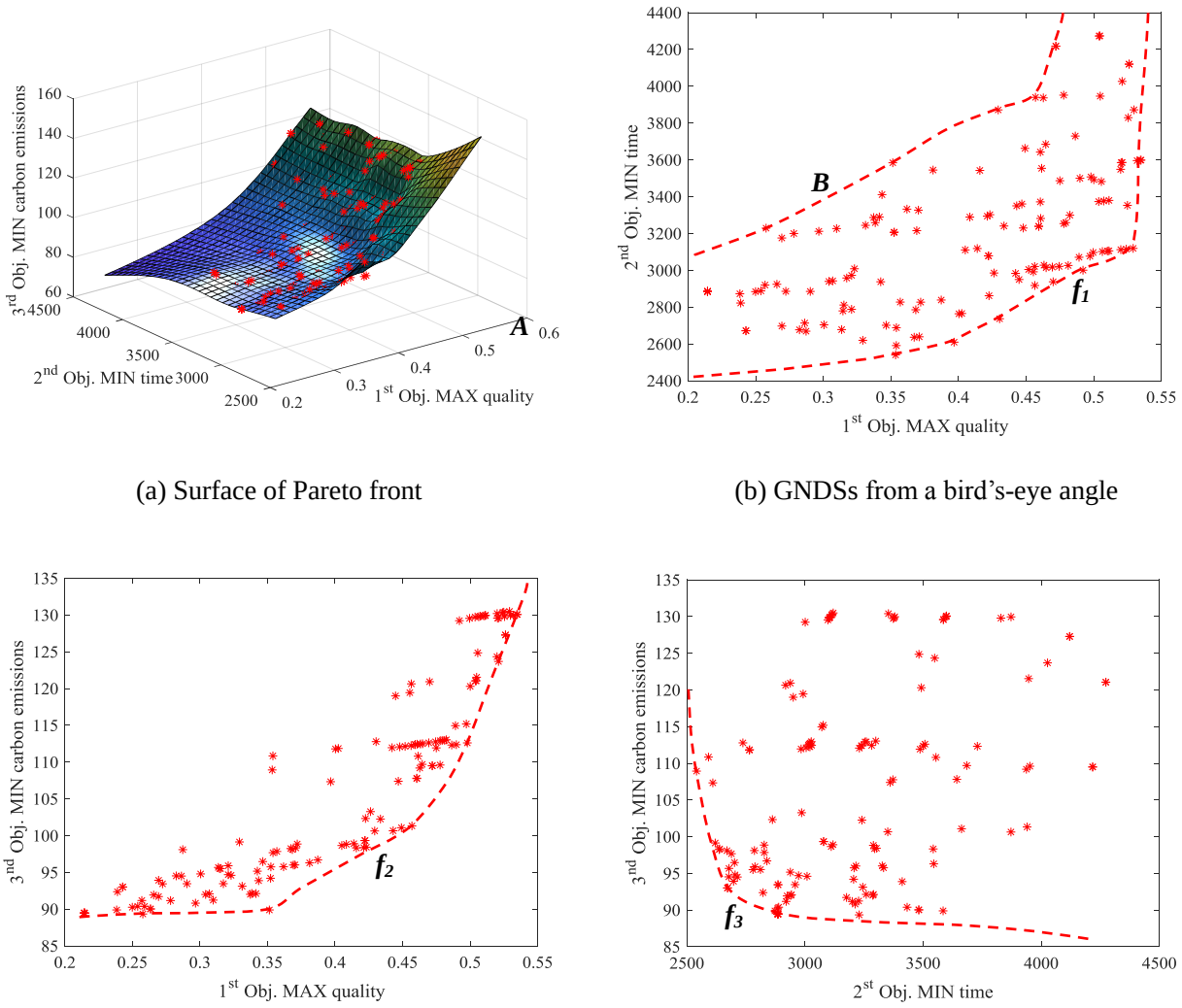

(a) Surface of Pareto front

(b) GNDSs from a bird's-eye angle

(c) GNDSs from a right-hand-side angle

(d) GNDSs from a left-hand-side angle

Fig. 5 Four scatterplots of GNDSs from different angles

By omitting one dimension from the original three-dimensional subfigure (i.e., Fig. 5a), some insights are gained. Figs. 5b-5d show the GNDS scatterplots from different angles of view. In these subfigures, we also draw Pareto fronts which we call "line of Pareto front" (LPF), and the star-shaped points in LPF is called "local NDSs" (LNDSs). Note that all star-shaped points in these subfigures are still the GNDSs, but not necessary the LNDSs in terms of the present subfigure. In Fig. 5b, the major part of the particle population is in the area between the LPF f_1 and an approximately-parallel line B, which means that the tradeoff between quality and time can be

achieved at different carbon-emission levels. However, it also implies that the DM can achieve a second-best tradeoff between quality and time when they must submit to an acceptable limitation on carbon emissions. This phenomenon conforms with the viewpoint of major literatures which highlight the environmental impact rather than other objectives.

Furthermore, Fig. 5c presents that the most GNDSs are close to LPF f_2, which means that the optimal tradeoff between quality and carbon emissions can make the timeliness well-realized. In other words, it is not advisable to sacrifice the interests of the quality and carbon emissions objectives to only meet the demand of timeliness. Unlike Figs. 5b and 5c, Fig. 5d shows an extreme condition in which most GNDSs do not care their distances from LPF f_3. This implies the reality that high quality is often not resulted from the best tradeoff between time and carbon emissions. Either time or carbon emissions has/have to make concessions in order to achieve a "high quality" goal.

Three managerial insights are generated as follows:

- The second-best tradeoff between quality and time can be achieved when given beforehand a reasonable carbon-emission limitation.
- The best tradeoff between quality and carbon emissions can ensure well-realized timeliness.
- The best tradeoff between time and carbon emissions cannot result in high quality.

5.3. Bayesian updates

5.3.1. Effects by Bayesian updates

As highlighted before, the proposed technology based on the Bayesian approach can explain the probabilistic changes of arc parameters after QIA decision making. We choose the GNDS which

is the closest to the ideal point A as an example. In this GNDS, QIAs are carried out in several nodes. Accordingly, totally ten arcs are Bayesian-updated by QIAs. We draw the joint probability density of time and carbon emissions for each arc, and obtain numerous bell-shaped surfaces. We then focus on the two metrics of each bell-shaped surface, i.e., the central location and the height. As shown in Fig. 6, the central locations of pre-update and post-update bells are distinctly different. The latter mostly are on further locations from the zero points than the former. We infer that the reason may lie in the employed QIA in each arc costs time and increases carbon emissions which respectively add(s) to the total time and energy consumption. Moreover, the post-update bells are much slimmer and taller than the pre-update ones, which indicates that Bayesian updates reduce the fluctuations of time and energy consumption. Therefore, two managerial insights are summed up as:

- The Bayesian approach evaluates the differences between the pre-update and post-update arc parameters.
- The Bayesian approach mitigates the instability of the post-update arc parameters.

5.3.2. Sensitivity analysis

Fig. 6 also conducts the sensitivity analysis on the effects of the uncertainty mitigation after we simulate QIA trials for different times ($N_{im} = 10, 20, 30, 40, 50$, respectively). More details are shown in Table 6. We obtain the following three managerial insights.

- The increase of the QIA-trial size lets the bells leave their current locations and move to new ones.
- The increase of the QIA-trial size gradually narrows the gap between the two neighbouring bells.
- The increase of the QIA-trial size leads to much slimmer and taller bells.

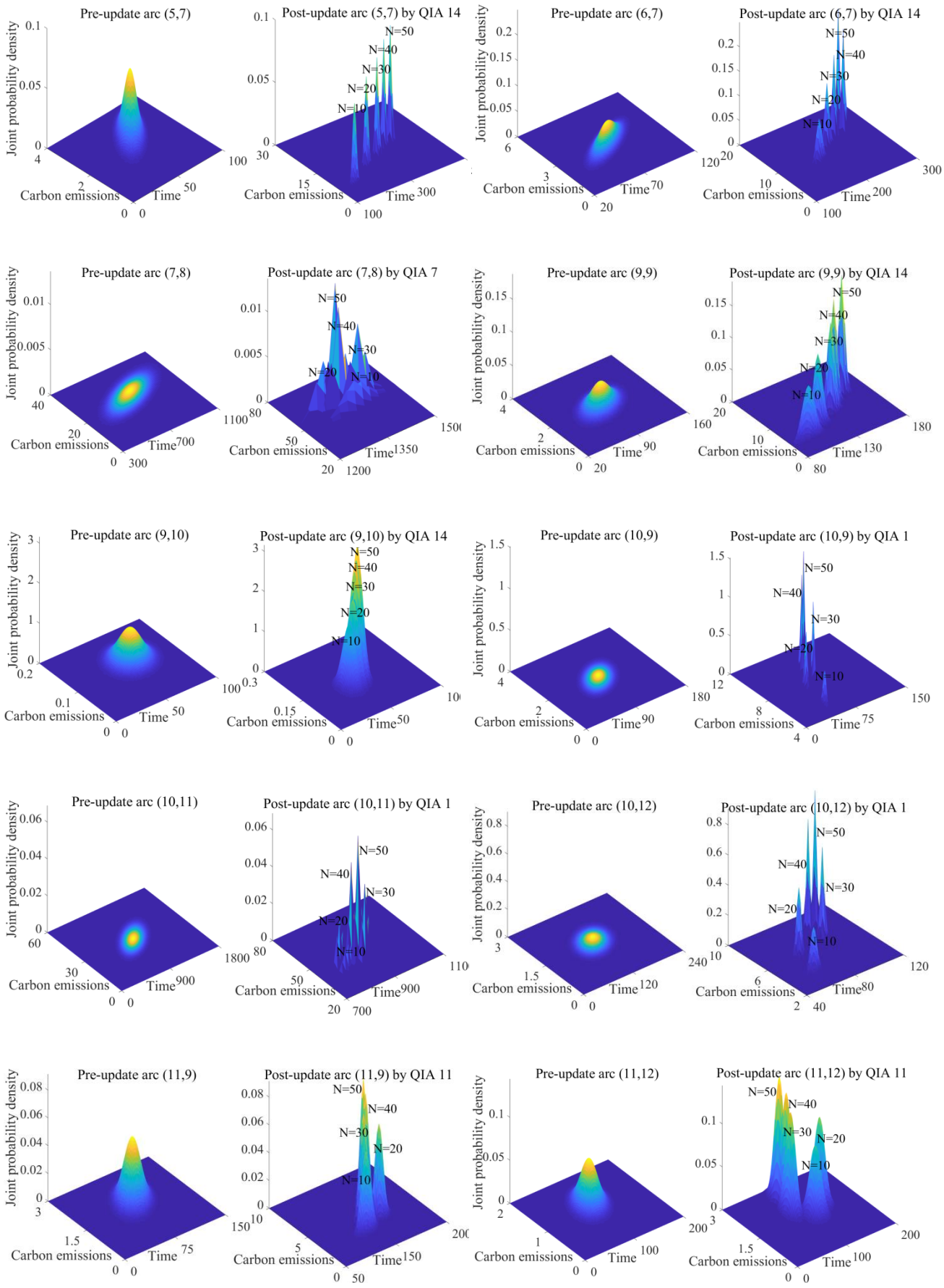

Fig. 6 Differences between pre- and post-update arc parameters

Table 6 Sensitivity analysis with respect to QIA-trial size

Arcs	*Change of QIA-trial size*	*Change of post-update parameters*				
		$\mu_{ij1\|im}$	$\mu_{ij2\|im}$	$\sigma_{ij1\|im}$	$\sigma_{ij2\|im}$	$\rho_{ij\|im}$
(5,7)	10	168.8	7.5749	9.2391	0.3959	0.7310
	20	243.8	10.7629	8.6610	0.3629	0.7068
	30	299.2	13.2635	8.1993	0.3370	0.6864
	40	346.4	14.5360	7.8175	0.3160	0.6688
	50	390.5	16.0089	7.4935	0.2985	0.6536
(6,7)	10	189.6	8.6441	7.7064	0.3651	0.7531
	20	219.8	10.6850	6.1331	0.3041	0.7467
	30	231.1	11.9956	5.2498	0.2664	0.7439
	40	250.7	12.7228	4.6644	0.2400	0.7425
	50	259.8	13.3442	4.2398	0.2203	0.7416
(7,8)	10	1239.7	48.8497	44.4649	1.7893	0.7646
	20	1381.3	52.1186	32.7648	1.3337	0.7737
	30	1335.0	54.7048	27.1494	1.1097	0.7769
	40	1328.7	55.0834	23.6908	0.9704	0.7786
	50	1373.5	55.8949	21.2877	0.8731	0.7797
(9,9)	10	108.7	4.2589	6.7039	0.3088	0.3894
	20	112.5	5.8745	5.0951	0.3001	0.4259
	30	141.8	7.6876	4.3181	0.2927	0.4583
	40	141.2	9.1999	3.8393	0.2861	0.4851
	50	135.6	10.7758	3.5061	0.2799	0.5074
(9,10)	10	49.0	0.1256	5.0649	0.0199	0.0836
	20	44.8	0.1315	3.8365	0.0198	0.0766
	30	60.9	0.1430	3.2129	0.0197	0.0752
	40	52.5	0.1488	2.8196	0.0196	0.0757
	50	38.8	0.1542	2.5427	0.0195	0.0771
(10,9)	10	52.9	5.5152	2.1868	0.2457	0.7331
	20	58.3	7.2894	1.7152	0.2104	0.7884
	30	64.8	8.8180	1.4741	0.1870	0.8110
	40	72.1	9.5134	1.3165	0.1700	0.8233
	50	73.1	9.9908	1.2020	0.1569	0.8310
(10,11)	10	835.8	39.0834	28.2474	1.3787	0.9582
	20	787.1	38.9648	20.3361	0.9939	0.9596
	30	802.7	41.3254	16.7070	0.8169	0.9601
	40	826.3	41.1083	14.5138	0.7099	0.9603
	50	806.3	40.9725	13.0059	0.6362	0.9604
(10,12)	10	67.9	4.1593	3.1269	0.2105	0.5396
	20	71.9	5.7211	2.3819	0.1878	0.6191
	30	79.3	7.1441	2.0301	0.1711	0.6574
	40	89.0	7.9069	1.8085	0.1583	0.6801
	50	90.4	8.4690	1.6503	0.1479	0.6950
(11,9)	10	156.6	3.0174	10.4154	0.2927	0.4286
	20	190.1	3.8673	8.9577	0.2888	0.4167
	30	162.1	4.2776	7.9929	0.2862	0.4129
	40	166.3	5.0710	7.2951	0.2842	0.4131
	50	172.6	5.5838	6.7607	0.2826	0.4156
(11,12)	10	149.0	1.6071	10.6628	0.1956	0.3037
	20	159.4	1.8750	8.5737	0.1942	0.2977
	30	101.7	1.9309	7.3853	0.1934	0.3013
	40	89.3	2.1933	6.5954	0.1929	0.3083
	50	93.1	2.3957	6.0226	0.1924	0.3166

The first and second insights can be explained by Property 1, while the third can be explained by Property 2. Property 1 states that the posterior mean is the weighted sum of the prior mean and the CMSM. The increase of the QIA-trial size, on one hand, impels the posterior mean to get closer to the CMSM because the QIA-trial size is proportional to the weight of the CMSM; and, on the other hand, makes the value of the CMSM more stable because the QIA-trial size is inversely proportional to the variance of the CMSM. Moreover, Property 2 states that the increase of the QIA-trial size broadens the gap between the posterior variance and the prior variance. Therefore, the bell will be more like a peak than its previous shape as QIA-trial size increases. In a word, the increase of the QIA-trial size reinforces the stability of the probabilistic change.

Nevertheless, the parameters' random nature remains, no matter which QIAs are carried out and how many arcs are Bayesian-updated. The time and carbon emissions still obey a joint probability distribution with the same type as the original. Therefore, when evaluating the probabilistic differences between pre-update and post-update arc parameters, an important advantage of our technology lies in that we only mitigates the uncertainty of arc parameters, but maintains the parameters with the random nature, which conforms to the complicated food spoilage mechanism.

5.4. Sustainable quality management plans

This part puts forward individualized sustainable quality management plans by different objective preferences. All GNDSs are first arranged respectively in descending/ascending/ascending order of their quality/time/carbon-emission objectives. As shown in Fig. 7, Nodes 1 and 2 coincidentally choose a simple food safety inspection technology when quality concern is highlighted. More specifically, Node 1 employs forage tests and Node 2 employs alcohol tests.

These two tests do not cost too much time and energy, but both can ensure a respectable quality improvement. However, Nodes 4, 5, 6, 7, 8, 9, and 11 all carry out more complex, multiple mechanized operations or food safety inspection technologies (Learning from Table 2, a QIA with a no-less-than-eleven number means the combined use of no-less-than-three operations or technologies) leading to more time and carbon emissions. This implies that:

- The raw-milk processing in Beingmate works well so that the milk quality is assured by deploying only simple milk safety inspection technologies.
- The DM shifts his focus to other steps (e.g., auxiliary materials concocting and sterilized bottles preparation) where quality assurance lags behind and potential hazard exists.

However, if the DM prefers the other two objectives, some time-consuming or carbon-intensive QIAs are replaced by time-saving or low-carbon ones. By comparing Figs. 8 and 9 with Fig. 7, Nodes 4, 7, 8, 9, and 11 in Fig. 7 reverse their QIA strategies in both Figs. 8 and 9 to simultaneously pursue time and energy savings. These nodes represent the assembling-related or recycling-related steps. QIA tradeoffs exist between quality and time (or carbon emissions) in these steps, such as using or not using filling machine, and improving or not improving recycling process. Unlike these steps, Nodes 5 and 6 still stick to the same QIA, which implies that those nodes associated with auxiliary materials concocting are in urgent need of QIA regardless of DM's preference on quality, time or carbon emissions. Therefore, the individualized sustainable quality management plans are node-oriented and objective-oriented. In this case, the nodes associated with the auxiliary materials concocting are given the highest priorities.

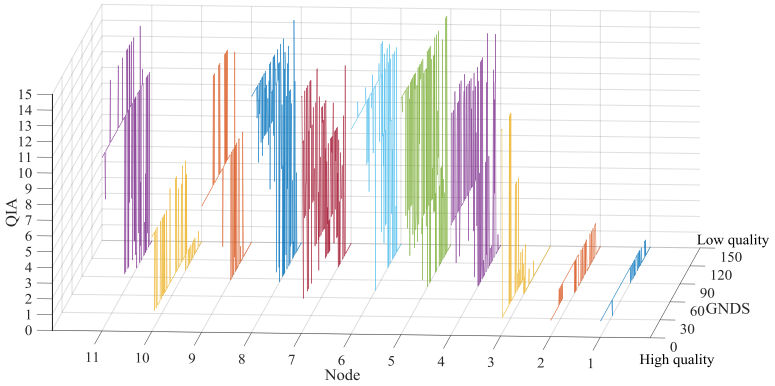

Fig. 7. QIA plans when highlighting quality concern

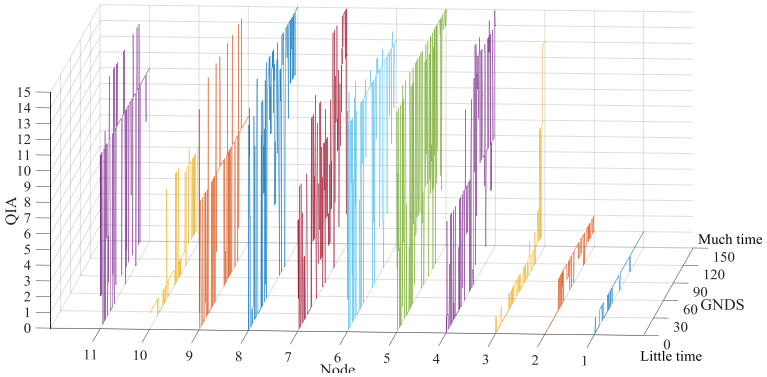

Fig. 8. QIA plans when highlighting timeliness concern

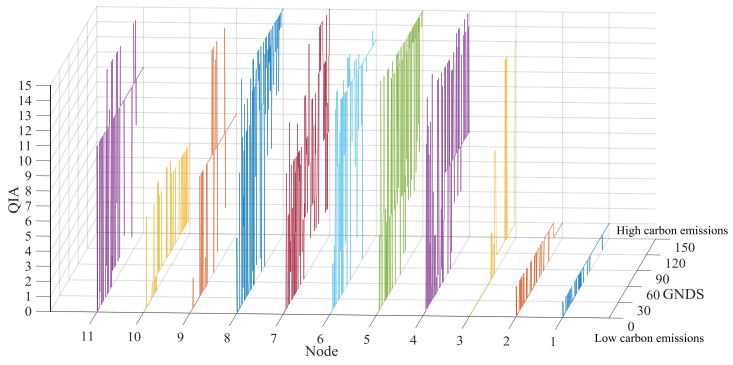

Fig. 9. QIA plans when highlighting carbon-emission concern

6. Conclusions

This study can be regarded as a tradeoff analysis on multi-dimensional components of food-production sustainability. The main innovation of this study is proposing a new technology by

implanting the Bayesian approach into the GERT, which is the first to use the above decision-making approach in food quality management. With the help of our technology, the dynamics and uncertainty can be jointly measured by the probabilistic difference between the pre-update and post-update status of food production networks. Or rather, our technology mitigates uncertainty, but it does not change the random nature of food production. This is a very important advantage of our technology, which conforms to the reality of food production systems and the complicated food spoilage mechanism involving a large number of uncertainties. Furthermore, the validity of our technology is based on plenty of historical data accumulation co-gathered by the firm and our affiliation. That is, our technology is data-driven, and not out of date.

Generally speaking, this study fills the gaps in the existing literatures. Besides the new technology highlighted above, the data source and model formulation are also unusual. Since we address QIA decision making on food production steps, the data are technology-based and mostly come from the food safety inspection, microbial tests, physicochemical tests, and so on. Fortunately, we have our own institute, laboratories, and funds to support this research. In our model, we have adopted a novel approach called CMOPSO to analyze the optimal tradeoffs of the three objectives. Our approach can visualize the optimal tradeoffs from different angles of view, and conclude the relationship between GDNS and LDNS. In addition, our approach can figure out individualized sustainable quality management plans, which are node-oriented and objective-oriented.

However, there are still some future research directions. First, we need to broaden our research scope to cover the whole product life cycle (not only food production) to put forward more thorough quality management plans, where the GERT networks are more complicated and the QIA candidates should be reconsidered. Second, we need to consider the effects of human behavioural

factors on the manual/mechanized use of the employed technologies in some QIAs. Third, we can combine our technology with the existing food-safety-related approaches, e.g., the HACCP system, to further explore hazard analysis and determine the critical control points for assurance of food safety. Nonetheless, we hope this study can be a beneficial supplement to the quality management field of perishable food with respect to technology innovation.

Acknowledgments

This work is supported by the National Natural Science Foundation of China (Grant No. 71603237, 71433006, 91746202, 71874158, 71403245), and Zhejiang Provincial Natural Science Foundation of China (Grant No. LY19G030004, LY17G020003). The authors thank the editors and anonymous reviewers for their thoughtful comments and constructive suggestions.

References

Akkerman, R., Farahani, P., Grunow, M., 2010. Quality, safety and sustainability in food distribution: A review of quantitative operations management approaches and challenges. *OR Spectrum* 32(4), 863–904.

Ala-Harja, H., Helo, P., 2014. Green supply chain decisions – Case-based performance analysis from the food industry. *Transportation Research Part E* 69, 97–107.

Albornoz, V.M., Urrutia–Gutiérrez, C., 2018. A mixed-integer linear optimization model for a two-echelon agribusiness supply chain. *Electronic Notes in Discrete Mathematics* 69, 253–260.

Allaoui, H., Guo, Y., Choudhary, A., Bloemhof, J., 2018. Sustainable agro-food supply chain design using two-stage hybrid multi-objective decision-making approach. *Computers & Operations Research* 89, 369–384.

Aras, N., Bilge, Ü., 2018. Robust supply chain network design with multi-products for a company

in the food sector. *Applied Mathematical Modelling* 60, 526–539.

Arnon-Rips, H., Poverenov, E., 2018. Improving food products' quality and storability by using Layer by Layer edible coatings. *Trends in Food Science & Technology* 75, 81–92.

Aschemann-Witzel, J., Giménez, A., Ares, G., 2018. Consumer in-store choice of suboptimal food to avoid food waste: The role of food category, communication and perception of quality dimensions. *Food Quality and Preference* 68, 29–39.

Aung, M.M., Chang, Y.S., 2014a. Temperature management for the quality assurance of a perishable food supply chain. *Food Control* 40, 198–207.

Aung, M.M., Chang, Y.S., 2014b. Traceability in a food supply chain: Safety and quality perspectives. *Food Control* 39, 172–184.

Baldwin, C., 2009. *Sustainability in the Food Industry*. John Wiley & Sons, New York.

Banasik, A., Kanellopoulos, A., Claassen, G.D.H., Bloemhof-Ruwaard, J.M., van der Vorst, J.G.A.J., 2017. Closing loops in agricultural supply chains using multi-objective optimization: A case study of an industrial mushroom supply chain. *International Journal of Production Economics* 183, 409–420.

Behzadi, G., O'Sullivan, M.J., Olsen, T.L., Zhang, A., 2018. Agribusiness supply chain risk management: A review of quantitative decision models. *Omega* 79, 21–42.

Berger, J.O., 1985. *Statistical Decision Theory and Bayesian Analysis*, second edition. Springer-Verlag.

Besik, D., Nagurney, A., 2017. Quality in competitive fresh produce supply chains with application to farmers' markets. *Socio-Economic Planning Sciences* 60, 62–76.

Bijma, F., Jonker, M., van der Vaart, A., 2017. *An Introduction to Mathematical Statistics*.

Amsterdam University Press.

Bolstad, W.M., Curran, J.M., 2017. *Introduction to Bayesian Statistics*, third edition. John Wiley & Sons.

Bortolini, M., Galizia, F.G., Mora, C., Botti, L., Rosano, M., 2018. Bi-objective design of fresh food supply chain networks with reusable and disposable packaging containers. *Journal of Cleaner Production* 184, 375–388.

Buisman, M.E., Haijema, R., Bloemhof-Ruwaard, J.M., 2019. Discounting and dynamic shelf life to reduce fresh food waste at retailers. *International Journal of Production Economics* 209, 274–284.

Chebolu-Subramanian, V., Gaukler, G.M., 2015. Product contamination in a multi-stage food supply chain. *European Journal of Operational Research* 244(1), 164–175.

Chernonog, T., Avinadav, T., 2019. Pricing and advertising in a supply chain of perishable products under asymmetric information. *International Journal of Production Economics* 209, 249–264.

Chen, C., Zhang, J., Delaurentis, T., 2014. Quality control in food supply chain management: An analytical model and case study of the adulterated milk incident in China. *International Journal of Production Economics* 152, 188–199.

Chen, Y.H., Huang, S., Mishra, A.K., Wang, X.H., 2018. Effects of input capacity constraints on food quality and regulation mechanism design for food safety management, *Ecological Modelling* 385, 89–95.

Dania, W.A.P., Xing, K., Amer, Y., 2018. Collaboration behavioural factors for sustainable agri-food supply chains: A systematic review. *Journal of Cleaner Production* 186, 851–864.

de Frias, J.A., Luo, Y., Zhou, B., Turner, E.R., Millner, P.D., Nou, X., 2018. Minimizing pathogen

growth and quality deterioration of packaged leafy greens by maintaining optimum temperature in refrigerated display cases with doors. *Food Control* 92, 488–495.

de Jong, P., 2013. *Sustainable Dairy Production*. John Wiley & Sons.

Ehrgott, M., 2005. *Multicriteria Optimization*, second edition. Springer Science & Business Media.

Feng, L., Chan, Y.L., Cárdenas-Barrón, L.E., 2017. Pricing and lot-sizing polices for perishable goods when the demand depends on selling price, displayed stocks, and expiration date. *International Journal of Production Economics* 185, 11–20.

Gillibert, R., Huang, J.Q., Zhang, Y., Fu, W.L., de La Chapelle, M.L., 2018. Food quality control by Surface Enhanced Raman Scattering. *Trends in Analytical Chemistry* 105, 185–190.

Govindan, K., 2018. Sustainable consumption and production in the food supply chain: A conceptual framework. *International Journal of Production Economics* 195, 419–431.

Govindan, K., Jafarian, A., Khodaverdi, R., Devika, K., 2014. Two-echelon multiple-vehicle location–routing problem with time windows for optimization of sustainable supply chain network of perishable food. *International Journal of Production Economics* 152, 9–28.

He, Z., Han, G., Cheng, T.C.E., Fan, B., Dong, J., 2018. Evolutionary food quality and location strategies for restaurants in competitive online-to-offline food ordering and delivery markets: An agent-based approach. *International Journal of Production Economics*, available online.

Hogg, R.V., Craig, A.T., 1978. *Introduction to Mathematical Statistics*, fourth edition. Macmillan Publishing Co., Inc.

Hsiao, Y.H., Chen, M.C., Chin, C.L., 2017. Distribution planning for perishable foods in cold chains with quality concerns: Formulation and solution procedure. *Trends in Food Science & Technology* 61, 80–93.

Huang, H., He, Y., Li, D., 2018. Pricing and inventory decisions in the food supply chain with production disruption and controllable deterioration. *Journal of Cleaner Production* 180, 280–296.

Irani, Z., Sharif, A.M., Lee, H., Aktas, E., Topaloğlu, Z., van't Wout, T., Huda, S., 2018. Managing food security through food waste and loss: Small data to big data. *Computers & Operations Research* 98, 367–383.

Jonkman, J., Barbosa-Póvoa, A.P., Bloemhof, J. M., 2019. Integrating harvesting decisions in the design of agro-food supply chains. *European Journal of Operational Research* 276(1), 247–258.

Jonkman, J., Bloemhof, J.M., Van der Vorst, J.G., van der Padt, A., 2017. Selecting food process designs from a supply chain perspective. *Journal of Food Engineering* 195, 52–60.

Kowalski, R.J., Li, C., Ganjyal, G.M., 2018. Optimizing twin-screw food extrusion processing through regression modeling and genetic algorithms. *Journal of Food Engineering* 234, 50–56.

Li, R., Chan, Y.L., Chang, C.T., Cárdenas-Barrón, L.E., 2017. Pricing and lot-sizing policies for perishable products with advance-cash-credit payments by a discounted cash-flow analysis. *International Journal of Production Economics* 193, 578–589.

Li, Y., Chu, F., Yang, Z., Calvo, R.W., 2016. A production inventory routing planning for perishable food with quality consideration. *IFAC-PapersOnLine* 49(3), 407–412.

Mangla, S.K., Luthra, S., Rich, N., Kumar, D., Rana, N.P., Dwivedi, Y.K., 2018. Enablers to implement sustainable initiatives in agri-food supply chains. *International Journal of Production Economics* 203, 379–393.

Miranda-Ackerman, M.A., Azzaro-Pantel, C., Aguilar-Lasserre, A.A., 2017. A green supply chain

network design framework for the processed food industry: Application to the orange juice agrofood cluster. *Computers & Industrial Engineering* 109, 369–389.

Mogale, D.G., Kumar, M., Kumar, S.K., Tiwari, M.K., 2018a. Grain silo location-allocation problem with dwell time for optimization of food grain supply chain network. *Transportation Research Part E* 111, 40–69.

Mogale, D.G., Kumar, S.K., Tiwari, M.K., 2018b. An MINLP model to support the movement and storage decisions of the Indian food grain supply chain. *Control Engineering Practice* 70, 98–113.

Moslemi, H., Zandieh, M., 2011. Comparisons of some improving strategies on MOPSO for multi-objective (r, Q) inventory system. *Expert Systems with Applications* 38(10), 12051–12057.

Musavi, M., Bozorgi-Amiri, A., 2017. A multi-objective sustainable hub location-scheduling problem for perishable food supply chain. *Computers & Industrial Engineering* 113, 766–778.

Ndraha, N., Hsiao, H.I., Vlajic, J., Yang, M.F., Lin, H.T.V., 2018. Time-temperature abuse in the food cold chain: Review of issues, challenges, and recommendations. *Food Control* 89, 12–21.

Nelson, R.G., Azaron, A., Aref, S., 2016. The use of a GERT based method to model concurrent product development processes. *European Journal of Operational Research* 250(2), 566–578.

Pritsker, A.A.B., 1966. GERT-Graphical evaluation and review technique. The RAND Corporation.

Rohmer, S.U.K., Gerdessen, J.C., Claassen, G.D.H., 2019. Sustainable supply chain design in the food system with dietary considerations: A multi-objective analysis. *European Journal of Operational Research* 273(3), 1149–1164.

Rong, A., Akkerman, R., Grunow, M., 2011. An optimization approach for managing fresh food

quality throughout the supply chain. *International Journal of Production Economics* 131(1), 421–429.

Sader, M., Pérez-Fernández, R., Kuuliala, L., Devlieghere, F., De Baets, B., 2018. A combined scoring and ranking approach for determining overall food quality. *International Journal of Approximate Reasoning* 100, 161–176.

Sel, C., Bilgen, B., Bloemhof-Ruwaard, J.M., van der Vorst, J.G., 2015. Multi-bucket optimization for integrated planning and scheduling in the perishable dairy supply chain. *Computers & Chemical Engineering* 77, 59–73.

Sgarbossa, F., Russo, I., 2017. A proactive model in sustainable food supply chain: Insight from a case study. *International Journal of Production Economics* 183, 596–606.

Shankar, R., Gupta, R., Pathak, D.K., 2018. Modeling critical success factors of traceability for food logistics system. *Transportation Research Part E* 119, 205–222.

Shen, Q., Zhang, J., Hou, Y.X., Yu, J.H., Hu, J.Y., 2018. Quality control of the agricultural products supply chain based on "Internet+". *Information Processing in Agriculture* 5(3), 394–400.

Singh, A., Shukla, N., Mishra, N., 2018. Social media data analytics to improve supply chain management in food industries. *Transportation Research Part E* 114, 398–415.

Soysal, M., Bloemhof-Ruwaard, J.M., van der Vorst, J.G.A.J., 2014. Modelling food logistics networks with emission considerations: The case of an international beef supply chain. *International Journal of Production Economics* 152, 57–70.

Stefansdottir, B., Depping, V., Grunow, M., Kulozik, U., 2018. Impact of shelf life on the trade-off between economic and environmental objectives: A dairy case. *International Journal of Production Economics* 201, 136–148.

Tabrizi, S., Ghodsypour, S.H., Ahmadi, A., 2018. Modelling three-echelon warm-water fish supply chain: A bi-level optimization approach under Nash–Cournot equilibrium. *Applied Soft Computing* 71, 1035–1053.

Teng, J.T., Cárdenas-Barrón, L.E., Chang, H.J., Wu, J., Hu, Y., 2016. Inventory lot-size policies for deteriorating items with expiration dates and advance payments. *Applied Mathematical Modelling* 40(19–20), 8605–8616.

Ting, S.L., Tse, Y.K., Ho, G.T.S., Chung, S.H., Pang, G., 2014. Mining logistics data to assure the quality in a sustainable food supply chain: A case in the red wine industry. *International Journal of Production Economics* 152, 200–209.

Tiwari, S., Cárdenas-Barrón, L.E., Goh, M., Shaikh, A.A., 2018. Joint pricing and inventory model for deteriorating items with expiration dates and partial backlogging under two-level partial trade credits in supply chain. *International Journal of Production Economics* 200, 16–36.

Tsang, Y.P., Choy, K.L., Wu, C.H., Ho, G.T.S., Lam, H.Y., Tang, V., 2018. An intelligent model for assuring food quality in managing a multi-temperature food distribution centre. *Food Control* 90, 81–97.

Utomo, D.S., Onggo, B.S., Eldridge, S., 2018. Applications of agent-based modelling and simulation in the agri-food supply chains. *European Journal of Operational Research* 269(3), 794–805.

Wang, J., Yue, H., 2017. Food safety pre-warning system based on data mining for a sustainable food supply chain. *Food Control* 73, 223–229.

Wang, J., Yue, H., Zhou, Z., 2017. An improved traceability system for food quality assurance and evaluation based on fuzzy classification and neural network. *Food Control* 79, 363–370.

Willersinn, C., Mack, G., Mouron, P., Keiser, A., Siegrist, M., 2015. Quantity and quality of food losses along the Swiss potato supply chain: Stepwise investigation and the influence of quality standards on losses. *Waste Management* 46, 120–132.

Yaseen, T., Sun, D.W., Cheng, J.H., 2017. Raman imaging for food quality and safety evaluation: Fundamentals and applications. *Trends in Food Science & Technology* 62, 177–189.

Yoo, S.H., Cheong, T., 2018. Quality improvement incentive strategies in a supply chain. *Transportation Research Part E* 114, 331–342.

Zhan, S.L., Liu, N., 2016. Determining the optimal decision time of relief allocation in response to disaster via relief demand updates. *International Journal of Systems Science* 47(3), 509–520.

Zhan, S.L., Liu, N., Ye, Y., 2014. Coordinating efficiency and equity in disaster relief logistics via information updates. *International Journal of Systems Science* 45(8), 1607–1621.

Zhang, G., Habenicht, W., Spieß, W.E.L., 2003. Improving the structure of deep frozen and chilled food chain with tabu search procedure. *Journal of Food Engineering* 60(1), 67–79.

Zhou, L., Xie, J., Gu, X., Lin, Y., Ieromonachou, P., Zhang, X., 2016. Forecasting return of used products for remanufacturing using Graphical Evaluation and Review Technique (GERT). *International Journal of Production Economics* 181, 315–324.